ETH ZURICH

MASTER THESIS

Gravitational waves from binaries on hyperbolic trajectories

Author:
Oliver Fischer

Supervisors:
Prof. Dr. Philippe Jetzer
Yannick Bötzel

A thesis submitted in fulfillment of the requirements for the degree of Master of Science

in the

Gravitation and Astrophysics Group
Department of Physics - University of Zurich

March 23, 2018

ETH ZURICH

Abstract

Department of Physics - ETH Zurich
Department of Physics - University of Zurich

Master of Science

Gravitational waves from binaries on hyperbolic trajectories

by Oliver Fischer

In this thesis we study gravitational waves emitted by hyperbolic encounters in terms of total emitted energy, the analytical power spectrum and the back-reaction effect on the trajectory. All calculations are done in the lowest order quradrupole approximation and carried out in much detail throughout this work. We also compare our results with the recent work done by García-Bellido and Nesseris [1] and in the parabolic limit $\epsilon = 1$ with the previous work done by Berry and Gair [2] for the case of elliptic orbits. We found that for a significantly strong enough interaction at the closest approach that the peak frequency of the power spectrum varies around a few 10Hz with strain amplitude of about 10^{-20}, which is observable by LIGO [3] . By considering a back-reaction effect on the trajectory we found that for critical impact parameters which lead to an initial eccentricity of $\epsilon \approx 1.05$ and lower that the eccentricity decreases to a value lower than 1 during the encounter, leading to a capture process.

Acknowledgements

Special thanks to Prof.Dr. Philippe Jetzer and Yannick Bötzel for the guidance through this work and the many helpful tips and discussions. And also thanks to Prof. Jetzer for all the interesting lectures on General Relativity in the last few semesters.

Contents

Physical Constants

Speed of Light	$c = 2.997\,924\,58 \times 10^{8}\,\mathrm{m\,s^{-1}}$
Gravitational Constant	$G = 6.674\,08 \times 10^{-11}\,\mathrm{m^{3}\,kg^{-1}\,s^{-2}}$
Solar Mass	$M_{\odot} = 1.988 \times 10^{30}\,\mathrm{kg}$
Astronomical Unit	$AU = 1.496 \times 10^{11}\,\mathrm{m}$
Parsec	$pc = 3.086 \times 10^{16}\,\mathrm{m}$

List of Symbols

Energy	E	J ($\mathrm{kg\,m^2\,s^{-2}}$)
Power	P	W ($\mathrm{J\,s^{-1}}$)
Angular Momentum	L	$\mathrm{kg\,m^2\,s^{-1}}$
Frequency	f	Hz ($\mathrm{s^{-1}}$)
Angular Frequency	$\omega = 2\pi f$	$\mathrm{rad\,s^{-1}}$
Impact Parameter	b	m
Impact Velocity	v_0	$\mathrm{m\,s^{-1}}$
Two Body Masses	m_1,m_2	kg
Total Mass	$m := m_1 + m_2$	kg
Reduced Mass	$\mu := \frac{m_1 \cdot m_2}{m}$	kg
	$\alpha := Gm\mu$	
Eccentricity	$\epsilon = \sqrt{1 + \frac{2EL^2}{\mu\alpha}}$	
Raidus at peri-astron	r_0	m
Angle at peri-astron	φ_0	rad
Metric Tensor	$g_{\mu\nu}$	
Ricci Tensor	$R_{\mu\nu}$	
Einstein Tensor	$G_{\mu\nu}$	
Energy-Momentum Tensor	$T_{\mu\nu}$	

Introduction

The theory of general relativity is now over 100 years old but still today the heart of our understanding of gravity. And it also took about 100 years until Einsteins predictions of the existence of gravitational waves was finally confirmed by the LIGO and Virgo Collaborations in 2016 [4] . On September 14, 2015 they detected the first gravitational signal coming from a binary black hole merger and opened a new door for experimental and theoretical astrophysics and cosmology. It was believed a long time that it is impossible to detect gravitational waves since the effect, the wave amplitude, is extremely small. But with the rapidly increasing level of expertise in engineering, theoretical work and data analysis it was nevertheless achieved to detect gravitational waves. The merger events, e.g. [4, 5], detected so far are gravitationally strong compared to signals coming from stable elliptic orbits or fly-by scenarios in the case for parabolic or hyperbolic trajectories and therefore easier to detect. Because of this fact most work done so far in this area is based on elliptic orbits and merger processes. In the future the precision may become high enough to look for much weaker processes like parabolic or hyperbolic encounters. Therefore it is useful to understand the gravitational wave emission from those encounters in much more detail. Our goal in this thesis is to give a derivation of the process of gravitational wave emission from hyperbolic encounters by finding the emitted energy, power, power spectrum and strain amplitude. We followed the procedure used by De Vittori, Jetzer and Klein [9] and corrected their results and give a detailed derivation. We also compare our results with the results found in previous works [1] and compare our parabolic limit with those based on studies of elliptic orbits [2, 8] . The calculations for the energy emission, power spectrum and back-reaction effect are carried out in much detail, either directly in the chapter or separately in the appendix.

To give a complete coherent overview of the topic the thesis is structured as follows: In the first chapter we briefly summarize the main steps going into the derivation of gravitational wave emission and we derive the quadrupole formula for the power emission. The second chapter clarifies the conventions for the geometry and the equations used here to describe hyperbolic trajectories. In the third chapter we study the power and energy emission for the concrete case hyperbolic encounters. The fourth chapter continues the study of power emission and we calculate the power spectrum of the gravitational wave emitted from a hyperbolic encounter. In the fifth chapter we consider eccentricity limits and compare the results found here with the ones calculated in previous papers on gravitational wave emission. In the last chapter we look at the back-reaction effect on the trajectory and with this in hand we understand qualitatively what leads to a capture process.

Chapter 1

Gravitational waves

Gravitational waves are found as solutions of the linearized field equations of General Relativity. This means that we assume a flat minkowski background metric and look at the evolution of small pertubations in space-time. In order to simplify the equations a bit more we use the low velocity approximation for source motions and the far zone approximation since we are mainly interested in observable effects at far distances from the source, e.g. on earth. A full derivation and discussion can be found in many good books on General Relativity and gravitational waves. Here we followed the book of Maggiore [7].

1.1 General description

We start by expanding the metric around flat minkowski space-time

$$g_{\mu\nu} = \eta_{\mu\nu} + h_{\mu\nu} \text{ with } |h_{\mu\nu}| \ll 1. \tag{1.1}$$

Plugging this expansion into the field equations and keep only terms of lowest order in $h_{\mu\nu}$ we get the following field equations for the perturbation

$$\Box \bar{h}_{\mu\nu} = -\frac{16\pi G}{c^4} T_{\mu\nu} \tag{1.2}$$

with

$$\bar{h}_{\mu\nu} := h_{\mu\nu} - \frac{1}{2} h \eta_{\mu\nu}. \tag{1.3}$$

In vacuum the field equation reduce to

$$\Box \bar{h}_{\mu\nu} = 0 \text{ with } \Box \equiv -\frac{1}{c^2}\partial_t^2 + \nabla^2. \tag{1.4}$$

Now we can introduce two gauge conditions to reduce the degrees of freedom from 10 to 2.

i. Lorentz gauge

$$\partial^\nu \bar{h}_{\mu\nu} = 0 \text{ gives } 10 \to 6 \text{ d.o.f.} \tag{1.5}$$

ii. Transverse traceless gauge (TT-gauge)

$$h^{0\mu} = 0 \tag{1.6}$$

$$h^i_i = 0 \text{ gives } 6 \to 2 \text{ d.o.f.} \tag{1.7}$$

outside the source.

Notice that the TT-gauge can only be chosen outside the source, since in this case the left-hand side of (1.2) vanishes and the Lorentz gauge does not fix the gauge completely. With the TT-gauge we perform another coordinate transformation which respects the Lorentz gauge and reduce the d.o.f. by another four.

We denote the gravitational wave tensor $h_{\mu\nu}$ in TT-gauge with $h^{TT}_{\mu\nu}$. For each component we can use a plane wave ansatz for the wave tensor in vacuum

$$h^{TT}_{ij}(\vec{x}) = e_{ij}(\vec{k})e^{i\vec{k}\vec{x}} \text{ with } \hat{n} = \frac{\vec{k}}{|\vec{k}|}. \tag{1.8}$$

Since we are interested in waves coming from a specific source we have to solve the field equations (1.2). This can be done by using Green's method giving

$$\bar{h}_{\mu\nu}(t,\vec{x}) = \frac{4G}{c^4}\int d^3x' \frac{1}{|\vec{x}-\vec{x}'|} T_{\mu\nu}(t - \frac{|\vec{x}-\vec{x}'|}{c}, \vec{x}'). \tag{1.9}$$

With the far zone approximation

$$|\vec{x}-\vec{x}'| = r - \vec{x}'\cdot\hat{n} + O(\frac{d^2}{r}) \tag{1.10}$$

and the TT-gauge projector $\Lambda_{ij,kl}(\hat{n})$ we arrive at

$$h^{TT}_{ij}(t,\vec{x}) = \frac{1}{r}\frac{4G}{c^4}\Lambda_{ij,kl}(\hat{n})\int d^3x' T_{kl}(t - \frac{r}{c} + \frac{\vec{x}'\cdot\hat{n}}{c}, \vec{x}'). \tag{1.11}$$

(1.11) is valid for relativistic and non-relativistic sources, as long as we are in the linearized theory and in the far zone approximation.

1.2 Energy and power of gravitational waves

In order to find the energy of a gravitational waves we have to take a more general ansatz for the metric expansion. We use a smooth background metric $\bar{g}_{\mu\nu}$ and distinguish between high frequency perturbation modes and low frequency background modes or equivalent short perturbation wave lengths and long source wave lengths. The general ansatz can be written as follows

$$g_{\mu\nu} = \bar{g}_{\mu\nu} + h_{\mu\nu} \text{ with } |h_{\mu\nu}| \ll 1. \tag{1.12}$$

We now make a size and frequency distinction:

i. Size

$$\lambda\!\!\!^{-} \ll L_B \tag{1.13}$$

ii. Frequency

$$f \ll f_B. \tag{1.14}$$

Now we use the Eintstein field equations

$$R_{\mu\nu} = \frac{8\pi G}{c^4}(T_{\mu\nu} - \frac{1}{2}g_{\mu\nu}T) \tag{1.15}$$

and expand $R_{\mu\nu}$ around the smooth background $\bar{g}_{\mu\nu}$ up to the order $O(h^2)$ and find

$$R_{\mu\nu} \approx \bar{R}_{\mu\nu} + R^{(1)}_{\mu\nu} + R^{(2)}_{\mu\nu}. \tag{1.16}$$

$\bar{R}_{\mu\nu}$ contains only background terms from $\bar{g}_{\mu\nu}$, $R^{(1)}_{\mu\nu}$ contains only high frequency terms from $h_{\mu\nu}$ and $R^{(2)}_{\mu\nu}$ contains high and low frequency terms from products like $h^{(1)}_{\mu\nu}h^{(2)}_{\mu\nu}$. Now we can arrange terms in (1.15) and find a low and a high frequency equation

$$\bar{R}_{\mu\nu} = -\left[R^{(2)}_{\mu\nu}\right]^{low} + \frac{8\pi G}{c^4}(T_{\mu\nu} - \frac{1}{2}g_{\mu\nu}T)^{low} \tag{1.17}$$

and

$$R^{(1)}_{\mu\nu} = -\left[R^{(2)}_{\mu\nu}\right]^{high} + \frac{8\pi G}{c^4}(T_{\mu\nu} - \frac{1}{2}g_{\mu\nu}T)^{high}. \tag{1.18}$$

The first equation will give us the energy momentum tensor of the gravitational wave and the second one describes its propagation. Now we use a common average procedure to filter the modes we are interested in. We choose the frequency representation and integrate over a certain time scale $\bar{t}$ such that $\frac{1}{f} \ll \bar{t} \ll \frac{1}{f_B}$, which we denote as $< ... >$. Now we can write

$$\bar{R}_{\mu\nu} = -\left\langle R^{(2)}_{\mu\nu}\right\rangle + \frac{8\pi G}{c^4}\left\langle T_{\mu\nu} - \frac{1}{2}g_{\mu\nu}T\right\rangle \tag{1.19}$$

and define the effective macroscopic energy momentum tensor of our matter source as

$$\left\langle \underbrace{T_{\mu\nu}}_{\text{microscopic}} - \frac{1}{2}g_{\mu\nu}T\right\rangle = \underbrace{\bar{T}_{\mu\nu}}_{\text{macroscopic}} - \frac{1}{2}\bar{g}_{\mu\nu}\bar{T}. \tag{1.20}$$

Furthermore we define

$$t_{\mu\nu} := -\frac{c^4}{8\pi G}\left\langle R^{(2)}_{\mu\nu} - \frac{1}{2}\bar{g}_{\mu\nu}R^{(2)}\right\rangle \leftrightarrow -\left\langle R^{(2)}_{\mu\nu}\right\rangle = \frac{8\pi G}{c^4}(t_{\mu\nu} - \frac{1}{2}\bar{g}_{\mu\nu}t), \tag{1.21}$$

which will be the energy momentum tensor of the gravitational wave. Putting things together we can write the dynamics of the background $\bar{g}_{\mu\nu}$ up to second order $O(h^2)$ as follows

$$\bar{R}_{\mu\nu} - \frac{1}{2}\bar{g}_{\mu\nu}\bar{R} = \frac{8\pi G}{c^4}\left(\underbrace{\bar{T}_{\mu\nu}}_{\text{matter}} + \underbrace{t_{\mu\nu}}_{\text{gravitational wave}}\right). \tag{1.22}$$

Using the explicit expansion in terms of $h_{\mu\nu}$ in the Lorentz gauge we find

$$t_{\mu\nu} = \frac{c^4}{32\pi G}\left\langle \partial_\mu h_{\alpha\beta}\partial_\nu h^{\alpha\beta}\right\rangle. \tag{1.23}$$

$t_{\mu\nu}$ is invariant under gauge transformation and therefore it is only determined by its physical modes and we can again use h^{TT}_{ij}. The energy is given by the 00-component

$$t^{00} = \frac{c^2}{32\pi G}\left\langle \dot{h}^{TT}_{ij}\dot{h}^{TT}_{ij}\right\rangle, \tag{1.24}$$

with $\dot{h} \equiv \partial_t h$. To find the power we start with the energy momentum conservation of $t^{\mu\nu}$

$$\partial_\mu t^{\mu\nu} = 0 \rightarrow \int_V d^3x(\partial_0 t^{00} + \partial_i t^{0i}) = 0. \tag{1.25}$$

This gives us

$$\partial_0 \int_V d^3x t^{00} = -\int_V d^3x \partial_i t^{i0} \tag{1.26}$$

$$\frac{1}{c}\frac{\partial E_V}{\partial t} = -\int_S dA n_i t^{0i} \tag{1.27}$$

and using spherical symmetry and the TT-gauge far from the source ($dA = r^2 d\Omega$ and $\hat{n} = \hat{r}$) we get

$$\partial_t E = -c\int_S dA t^{0r} \text{ with } t^{0r} = \left\langle \partial^0 h_{ij}^{TT} \partial_r h_{ij}^{TT} \right\rangle. \tag{1.28}$$

For a spherical symmetric gravitational wave traveling in the radial direction we can assume the general form at large distances

$$\partial_r h_{ij}^{TT} = \frac{1}{r} f_{ij}(t - \frac{r}{x}) \rightarrow t^{00} = +t^{0r}. \tag{1.29}$$

For the energy flux we therefore get

$$\frac{dE}{dAdT} = +ct^{00}. \tag{1.30}$$

Since E_V, the energy inside the volume V, decreases the gravitational wave will carry away the energy E. The power $P = \frac{dE}{dt}$ is then given by

$$\frac{dE}{dt} = \frac{c^3 r^2}{32\pi G}\int d\Omega \left\langle \dot{h}_{ij}^{TT} \dot{h}_{ij}^{TT} \right\rangle. \tag{1.31}$$

To proceed further we will consider (1.11), in the low velocity approximation for a non-relativistic source. Let ω_s be the average internal frequency of the source and d its typical size than $v \propto \omega_s d$ is the typical internal velocity. For a non-relativistic source we will assume that $v \ll c$. Consider now the following Fourier transformation for T_{kl}.

$$T_{kl}\left(t - \frac{r}{c} + \frac{\vec{x}' \cdot \hat{n}}{c}, \vec{x}'\right) = \int \frac{d^4k}{(2\pi)^4} \tilde{T}_{kl}(w, \vec{k}) e^{-i\omega(t - r/c + \vec{x}' \cdot \hat{n}/c) + i\vec{k} \cdot \vec{x}'}. \tag{1.32}$$

Using the low velocity approximation $\frac{\omega}{c}\vec{x}' \cdot \hat{n} \leq \frac{\omega_S d}{c} \ll 1$ we can expand the exponential above as

$$e^{-i\omega(t - r/c + \vec{x}' \cdot \hat{n}/c)} \approx e^{-i\omega(t - r/c)}\left(1 - i\frac{w}{c}x'^i n + \frac{1}{2}(-i\frac{w}{c})^2 x'^i x'^j n^i n^j + ...\right). \tag{1.33}$$

This will be equivalent to

$$T_{kl}\left(t - \frac{r}{c} + \frac{\vec{x}' \cdot \hat{n}}{c}, \vec{x}'\right) \approx T_{kl}\left(t - \frac{r}{c}, \vec{x}'\right) + \frac{x'^i n^i}{c}\partial_0 T_{kl} + \frac{1}{2c^2} x'^i x^j n^i n^j \partial_0^2 T_{kl} + ... \tag{1.34}$$

evaluated at $(t - r/c, \vec{x}')$. To simplify the notation and to get a deeper inside into the physical meaning of different terms we introduce the following set of momenta for the energy

momentum tensor T_{ij}

$$S^{ij} = \int d^3x T^{ij}(t,\vec{x}), \tag{1.35}$$

$$S^{ij,k} = \int d^3x T^{ij}(t,\vec{x})x^k, \tag{1.36}$$

$$S^{ij,kl} = \int d^3x T^{ij}(t,\vec{x})x^k x^l. \tag{1.37}$$

Using these momenta we can write down the gravitational wave tensor in a more compact form

$$h_{ij}^{TT} = \frac{1}{r}\frac{4G}{c^4}\Lambda_{ij,kl}(\hat{n})\left[\underbrace{S^{kl}}_{O(1)} + \underbrace{\frac{n_m}{c}\dot{S}^{kl,m}}_{O(v/c)} + \underbrace{\frac{n_m n_p}{c^2}\ddot{S}^{kl,mp}}_{O(v^2/c^2)} + ...\right]_{(t-r/c,\vec{x})} \tag{1.38}$$

and clearly see how the order increases term by term. Furthermore we can introduce momenta for the energy density T^{00} and the linear momentum T^{0i}

$$\begin{aligned} M &= \frac{1}{c^2}\int d^3x T^{00}(t,\vec{x}) & P^i &= \frac{1}{c}\int d^3x T^{0i}(t,\vec{x}) \\ M^i &= \frac{1}{c^2}\int d^3x T^{00}(t,\vec{x})x^i & P^{i,j} &= \frac{1}{c}\int d^3x T^{0i}(t,\vec{x})x^j \\ M^{ij} &= \frac{1}{c^2}\int d^3x T^{00}(t,\vec{x})x^i x^j & P^{i,jk} &= \frac{1}{c}\int d^3x T^{0i}(t,\vec{x})x^j x^k. \end{aligned} \tag{1.39}$$

Using the energy momentum conservation in the linearized theory we find

$$\partial_\mu T^{\mu\nu} = 0 \quad \Rightarrow \quad \begin{aligned} \dot{M} &= 0 \leftrightarrow \text{ Mass conservation} \\ \dot{P}^i &= 0 \leftrightarrow \text{ Momentum conservation} \\ S^{ij} &= \frac{1}{2}\ddot{M}_{ij}. \end{aligned} \tag{1.40}$$

To lowest order we finally find the formula for the mass quadrupole radiation wavetensor

$$\left[h_{ij}^{TT}\right]_{quad} = \frac{1}{r}\frac{4G}{c^4}\Lambda_{ij,kl}(\hat{n})\ddot{M}_{ij}(t-\frac{r}{c}). \tag{1.41}$$

By defining the tracefree quadrupole moment

$$D_{ij} \equiv 3M_{ij} - \delta_{ij}M_{kk} \tag{1.42}$$

we can also write

$$\left[h_{ij}^{TT}\right]_{quad} = \frac{1}{r}\frac{2G}{c^4}\ddot{D}_{ij}^{TT}(t-\frac{r}{c}). \tag{1.43}$$

Using (1.31) and integrate over $d\Omega$ we find the quadrupole formula for the power

$$P_{quad} = \frac{G}{45c^5}\left\langle \dddot{D}_{ij}\dddot{D}_{ij}\right\rangle. \tag{1.44}$$

Chapter 2

Hyperbolic encounters

2.1 General geometry and equations

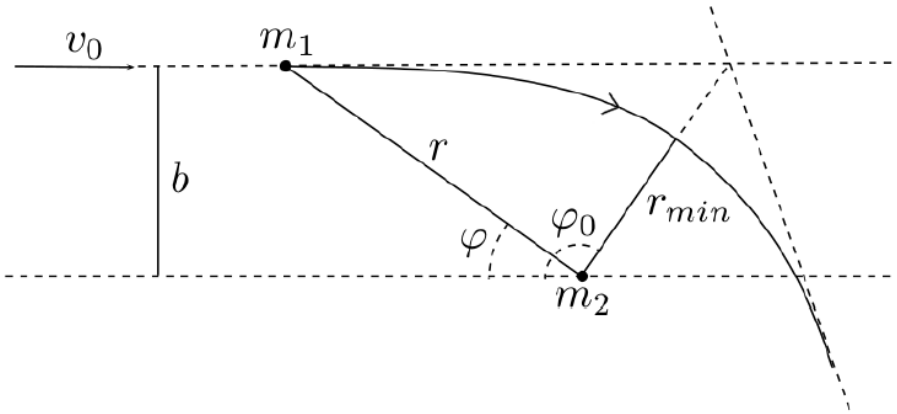

FIGURE 2.1: Geometry of a hyperbolic encounter.
Convention used by De Vittori,Jetzer and Klein [8].

The general geometry of a hyperbolic encounter is given in figure 2.1. The two body problem can be rewritten into an one body problem using the reduced mass μ and to simplify the equation further we use also polar coordinates (r, φ) in the orbital plane, since the motion is restricted to $x-y-$plane due to constant angular momentum L. The energy and angular momentum of the system in terms of polar coordinates are than given by:

$$E = T + V = \frac{1}{2}\mu\dot{\vec{r}}^2 + V(r) = \frac{\mu}{2}(\dot{r}^2 + r^2\dot{\varphi}^2) + V(r) = const. \tag{2.1}$$

$$L = |\vec{L}| = \mu r^2\dot{\varphi} = const. \tag{2.2}$$

with potential

$$V(r) = -\frac{Gm_1m_2}{r}. \tag{2.3}$$

Solving 2.1 for $r(\varphi)$ we find:

$$r(\varphi) = \frac{a(\epsilon^2 - 1)}{1 + \epsilon\cos(\varphi - \varphi_0)} \tag{2.4}$$

where we introduced the following abbreviations:

$$a := \frac{\alpha}{2E}, \tag{2.5}$$

$$\alpha := Gm\mu, \tag{2.6}$$

$$\text{Eccentricity } \epsilon := \sqrt{1 + \frac{2EL^2}{\mu\alpha^2}}, \tag{2.7}$$

with

$$\begin{array}{ll} \text{Total mass} & \mathrm{m} := m_1 + m_2, \\ \text{Reduced mass} & \mu := \frac{m_1 m_2}{m}. \end{array}$$

For the the special case of a hyperbolic encounter E and L can be written in terms of impact parameter b and impact velocity v_0 as follows:

$$L = \mu b v_0, \tag{2.8}$$

$$E = \frac{1}{2}\mu v_0^2 \tag{2.9}$$

$$\tag{2.10}$$

and therefore

$$\epsilon = \epsilon(v_0, b, m) = \sqrt{1 + \frac{v_0^4 b^2}{G^2 m^2}}, \tag{2.11}$$

$$a = \frac{Gm}{v_0^2}, \tag{2.12}$$

with φ_0 the angle related to the minimal distance r_0 and given by the following relation

$$\epsilon = -\frac{1}{\cos(\varphi_0)}. \tag{2.13}$$

An alternative for (2.4) is given and used in [6] is

$$r(\varphi) = \frac{b\sin(\varphi_0)}{\cos(\varphi - \varphi_0) - \cos(\varphi_0)}. \tag{2.14}$$

For later calculations it is also usefull to introduce the eccentric anomaly ξ to find the following parametrization for hyperbolic trajectories

$$t = \sqrt{\frac{\mu a^3}{\alpha}}(\epsilon\sinh(\xi) - \xi) = \eta(\epsilon\sinh(\xi) - \xi) \tag{2.15}$$

$$r = a(\epsilon\cosh(\xi) - 1) \tag{2.16}$$

$$\tan(\frac{\varphi - \varphi_0}{2}) = \sqrt{\frac{\epsilon + 1}{\epsilon - 1}}\tanh(\frac{\xi}{2}) \tag{2.17}$$

$$x = a(\epsilon - \cosh(\xi)) \tag{2.18}$$

$$y = a\sqrt{\epsilon^2 - 1}\sinh(\xi). \tag{2.19}$$

Chapter 3

Gravitational wave power and energy from hyperbolic encounters

3.1 Power and energy in the quadrupole approximation

The power of a gravitational wave in the lowest order approximation is given in (1.44) as

$$P_{quad} = \frac{G}{45c^5}\langle \dddot{D}_{ij}\dddot{D}_{ij}\rangle \tag{3.1}$$

where D_{ij} is the tracefree quadrupole moment

$$D_{ij} = 3M_{ij} - \delta_{ij}M_{kk} \tag{3.2}$$

and M_{ij} is the mass quadrupole moment of the reduced mass given by

$$M_{ij} = \frac{1}{c^2}\int T^{00}x_i x_j d^3x, \tag{3.3}$$

with the 00-component of the energy momentum tensor given by

$$T^{00} = \mu\delta(\vec{x} - \vec{x}')c^2. \tag{3.4}$$

We can now use polar coordinates (r, φ) to write down the M_{ij} momenta

$$M_{11} = \mu x^2 = \mu r(\varphi)^2\cos^2(\varphi) \tag{3.5}$$
$$M_{11} = \mu y^2 = \mu r(\varphi)^2\sin^2(\varphi) \tag{3.6}$$
$$M_{12} = M_{21} = \mu xy = \mu r(\varphi)^2\cos(\varphi)\sin(\varphi) \tag{3.7}$$
$$M_{i3} = M_{3j} = 0. \tag{3.8}$$
$$\tag{3.9}$$

Using the explicit expression (3.2) in (3.1) we find

$$P_{quad} = \frac{G}{45c^5}6\langle \dddot{M}_{11}^2 + \dddot{M}_{22}^2 + 3\dddot{M}_{12}^2 - \dddot{M}_{11}\dddot{M}_{22}\rangle. \tag{3.10}$$

We can calculate the third time derivatives of the momenta in (3.10) and simplify the expression for P_{quad}. Using the time parametrization we find

$$P_{quad}(\xi) = \frac{G}{45c^5}6\frac{2a^4\mu^2(-24 + 23\epsilon^2 + \epsilon^2\cosh(2\xi))}{n^6(-1 + \epsilon\cosh(\xi))^6} \tag{3.11}$$

where the φ-ξ-relation is given in (2.15). Using the r-φ representation we find

$$P_{quad}(\varphi) = \frac{32GL^6}{45c^5b^8\mu^4} f(\varphi, \varphi_0) \tag{3.12}$$

with

$$f(\varphi, \varphi_0) = \frac{\sin(\frac{\varphi}{2} - \varphi_0)^4 \sin(\frac{\varphi}{2})^4}{\tan(\varphi_0)^2 \sin(\varphi_0)^6} (150 + 72\cos(2\varphi_0) + 66cos(2\varphi_0 - 2\varphi) \\ -144(\cos(\varphi - 2\varphi_0) + \cos(\varphi))). \tag{3.13}$$

To find the total energy released during the encounter we need to perform a time integral of (3.10) over $\mathbb{R}$

$$E_{tot} = \int_{\mathbb{R}} \left| \frac{dE}{dt} \right| = \int_{\mathbb{R}} |P| dt. \tag{3.14}$$

Since P is given as a function of φ we perform a change of variables using (2.2)and integrate over the trajectory with $\varphi \in (0, 2\varphi_0)$ which gives

$$E_{tot} = \frac{\mu}{L} \int_0^{2\varphi_0} P_{quad}(\varphi) r(\varphi)^2 d\varphi. \tag{3.15}$$

Performing the integral we find

$$E_{tot} = \frac{GL^5}{90b^6c^5\mu^3} F(\varphi_0) \tag{3.16}$$

with

$$F(\varphi_0) = \frac{1}{\tan(\varphi_0)^2 \sin(\varphi_0)^4} (2628\varphi_0 + 2328\varphi_0 \cos(2\varphi_0) + 144\varphi_0 \cos(4\varphi_0) \\ -1948 \sin(2\varphi_0) - 301 \sin(4\varphi_0)). \tag{3.17}$$

A quick unit check for (3.11) ,(3.12) and (3.16) gives:

$$\left[\frac{Ga^4\mu^2}{c^5n^6}\right] = \left[\frac{\mu^2}{m^2} \frac{v_0^{10}}{c^5} \frac{1}{G}\right] = \frac{kg^2}{kg^2} \frac{\frac{m^{10}}{s^{10}}}{\frac{m^5}{s^5}} \frac{kg \cdot s}{m^3} = \frac{kg \cdot m^2}{s^3} = W = [P] \tag{3.18}$$

$$\left[\frac{GL^6}{c^5b^8\mu^4}\right] = \frac{m^3}{kg \cdot s^2} \frac{s^5}{m^5} \frac{kg^6 \cdot m^{12}}{s^6} \frac{1}{m^8} \frac{1}{kg^4} = \frac{kg \cdot m^2}{s^3} = W = [P] \tag{3.19}$$

$$\left[\frac{GL^5}{c^5b^6\mu^3}\right] = \frac{m^3}{kg \cdot s^2} \frac{kg^5 \cdot m^{10}}{s^5} \frac{s^5}{m^5} \frac{1}{m^6} \frac{1}{kg^3} = \frac{kg \cdot m^2}{s^2} = J = [E]. \tag{3.20}$$

So all prefactors fulfill the physical meaning of the respective expression calculated. If we plot both powerfunctions normalized with φ_0, see figure (3.1), we notice that the angular parts are consistent. We also see that we get a clear peak at φ_0 which is the turning point of the hyperbolic trajectory. Including the prefactors we find figure (3.2).

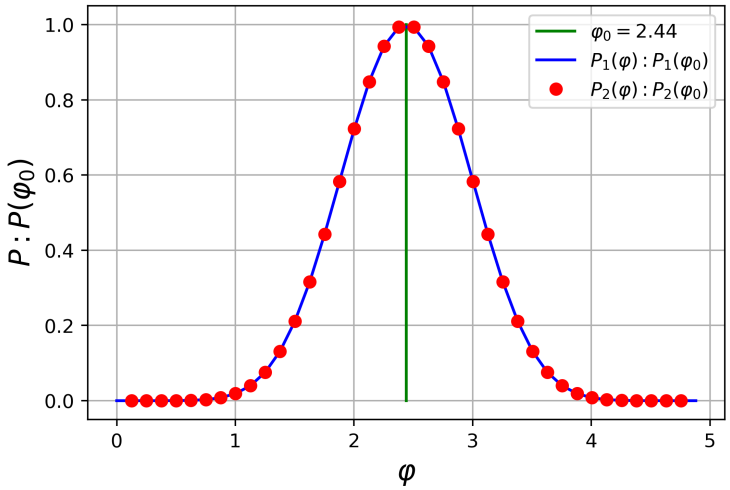

FIGURE 3.1: Normalized power for $\epsilon \approx 1.31$
P_1 and P_2 correspond to 3.12 and 3.11

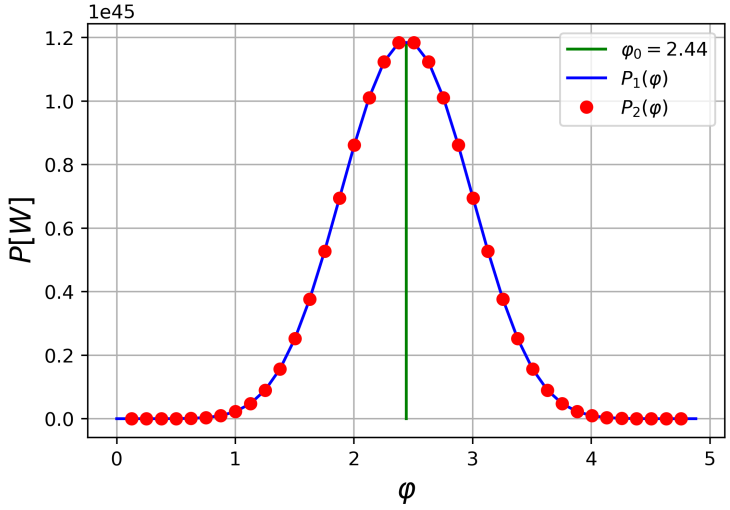

FIGURE 3.2: Power for $\epsilon \approx 1.31$

Chapter 4

Power spectrum from hyperbolic encounters

4.1 Power spectrum for an hyperbolic encounter

We will use the following Fourier transformation convention for all following calculations

$$f(t) = \frac{1}{2\pi}\int_{\mathbb{R}} \hat{f}(\omega)e^{-i\omega t}d\omega \tag{4.1}$$

$$\hat{f}(\omega) = \int_{\mathbb{R}} f(t)e^{i\omega t}dt \tag{4.2}$$

with

$$\delta(\omega-\omega') = \frac{1}{2\pi}\int_{\mathbb{R}} e^{-i(\omega-\omega')t}dt. \tag{4.3}$$

This convention gives us the following Parseval identity, see appendix A,

$$\int_{-\infty}^{+\infty} |f(t)|^2\, dt = \int_0^{+\infty} \frac{\left|\hat{f}(\omega)\right|^2}{\pi} d\omega. \tag{4.4}$$

To find the power spectrum we consider again the total energy for an hyperbolic encounter

$$\begin{aligned} E_{tot} &= \int_{-\infty}^{+\infty} P(t)dt = \int_{-\infty}^{+\infty} \frac{G}{45c^5}\langle \dddot{D}_{ij}\dddot{D}_{ij}\rangle dt \\ &= \int_{-\infty}^{+\infty} \frac{G}{45c^5}\left(\left|\dddot{D}_{11}(t)\right|^2 + \left|\dddot{D}_{22}(t)\right|^2 + 2\left|\dddot{D}_{12}(t)\right|^2 + \left|\dddot{D}_{33}(t)\right|^2\right) dt \\ &\overset{(4.4)}{=} \frac{1}{\pi}\int_{-\infty}^{+\infty} \frac{G}{45c^5}\left(\left|\widehat{\dddot{D}}_{11}(\omega)\right|^2 + \left|\widehat{\dddot{D}}_{22}(\omega)\right|^2 + 2\left|\widehat{\dddot{D}}_{12}(\omega)\right|^2 + \left|\widehat{\dddot{D}}_{33}(\omega)\right|^2\right) d\omega \\ &= \frac{1}{\pi}\int_0^{+\infty} P(\omega)d\omega, \end{aligned} \tag{4.5}$$

where the power spectrum $P(\omega)$ is given by

$$P(\omega) := \frac{G}{45c^5}\sum_{(ij)}\left|\widehat{\dddot{D}}_{ij}(\omega)\right|^2. \tag{4.6}$$

To find the trace free mass momenta D_{ij} we use again (2.15). For the non-zero momenta we get

$$\begin{aligned} D_{11} &= 2M_{11} - M_{22} \\ &= \frac{1}{2}a^2\mu\left((3-\epsilon^2)\cosh(2\xi) - 8\epsilon\cosh(\xi) + 1 + 5\epsilon\right) \qquad (4.7) \\ D_{22} &= 2M_{11} - M_{22} \\ &= \frac{1}{2}a^2\mu\left(4\epsilon\cosh(\xi) - 3\cosh(2\xi) + 2\epsilon^2 cosh(2\xi) + 1 - 4\epsilon^2\right) \qquad (4.8) \\ D_{33} &= -(M_{11} + M_{22}) \\ &= \frac{1}{2}a^2\mu\left(4\epsilon\cosh(\xi) - \epsilon^2\cosh(2\xi) - 2 - \epsilon^2\right) \qquad (4.9) \\ D_{12} &= D_{21} = 3M_{12} \\ &= \frac{1}{2}a^2\mu\sqrt{\epsilon^2-1}\left(6\epsilon\sinh(\xi) - 3\sinh(2\xi)\right). \qquad (4.10) \end{aligned}$$

Since we will only need third order time derivatives (∂_t^3) we can perform a constant coordinate shift which leaves the momenta invariant, see appendix B, and therefore we can ignore all constant terms in the above equations. So we are left with

$$\begin{aligned} D_{11} &= \frac{1}{2}a^2\mu\left((3-\epsilon^2)\cosh(2\xi) - 8\epsilon\cosh(\xi)\right) \qquad (4.11) \\ D_{22} &= \frac{1}{2}a^2\mu\left(4\epsilon\cosh(\xi) - 3\cosh(2\xi) + 2\epsilon^2 cosh(2\xi)\right) \qquad (4.12) \\ D_{33} &= \frac{1}{2}a^2\mu\left(4\epsilon\cosh(\xi) - \epsilon^2\cosh(2\xi)\right) \qquad (4.13) \\ D_{12} &= D_{21} = \frac{1}{2}a^2\mu\sqrt{\epsilon^2-1}\left(6\epsilon\sinh(\xi) - 3\sinh(2\xi)\right). \qquad (4.14) \end{aligned}$$

Using the time derivative properties of the Fourier transformation $\hat{f}^{(n)}(\omega) = (-i\omega)^n\hat{f}(\omega)$, see appendix A, the expression for the power spectrum (4.6) simplifies to

$$P(\omega) = \frac{G}{45c^5}\omega^6\sum_{(ij)}\left|\widehat{D}_{ij}(\omega)\right|^2 \qquad (4.15)$$

and we are left with the calculation of all $\widehat{D}_{ij}(\omega)$ using the expressions given above. A full calculation is done in appendix C. Using these we can write the sum in the previous expression as

$$\begin{aligned} \sum_{(ij)}\left|\widehat{D}_{ij}(\omega)\right|^2 &= \left|\widehat{D}_{11}(\omega)\right|^2 + \left|\widehat{D}_{22}(\omega)\right|^2 + \left|\widehat{D}_{33}(\omega)\right|^2 + 2\left|\widehat{D}_{12}(\omega)\right|^2 \\ &= \frac{1}{4}a^4\mu^2 16\pi^2\frac{\eta^2}{\nu^2}F_\epsilon(z) \end{aligned} \qquad (4.16)$$

with

$$\begin{aligned} F_\epsilon(z) = &\left|\frac{3(\epsilon^2-1)}{\epsilon}H_{i\nu}^{(1)\prime}(z) + \frac{(\epsilon^2-3)}{\epsilon^2}\frac{i}{\nu}H_{i\nu}^{(1)}(z)\right|^2 \\ &+ \left|\frac{3(\epsilon^2-1)}{\epsilon}H_{i\nu}^{(1)\prime}(z) + \frac{(2\epsilon^2-3)}{\epsilon^2}\frac{i}{\nu}H_{i\nu}^{(1)}(z)\right|^2 \\ &+ \left|\frac{i}{\nu}H_{i\nu}^{(1)}(z)\right|^2 \\ &+ 18\frac{(\epsilon^2-1)}{\epsilon^2}\left|\frac{(\epsilon^2-1)}{\epsilon}iH_{i\nu}^{(1)}(z) + \frac{1}{\nu}H_{i\nu}^{(1)\prime}(z)\right|^2 \end{aligned} \tag{4.17}$$

where $z \equiv i\nu\epsilon$. Using $\eta = \sqrt{a^3/Gm}$ and $\omega = \nu/\eta$ can write

$$P(\omega) = \frac{G^3M^2\mu^2}{a^2c^5}\frac{16\pi^2}{180}\nu^4 F_\epsilon(z). \tag{4.18}$$

$P(\omega)$ can be plotted for different eccentricities ϵ as shown in figure 4.1.

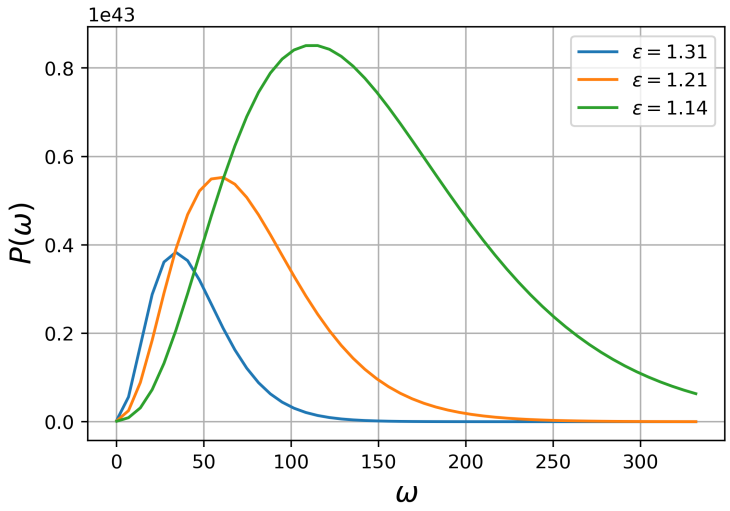

FIGURE 4.1: Power spectrum for different values of ϵ

4.2 Numerical evaluation

The total energy is given by

$$E_{tot} = \frac{1}{\pi}\int_0^\infty P(\omega)d\omega = \frac{G^{7/2}m^{5/2}\mu^2}{a^{7/5}c^5}\frac{16\pi}{180}\int_0^\infty \nu^4 F_\epsilon(i\nu\epsilon)d\nu. \tag{4.19}$$

We can evaluate this expression using numerical integration* and compare it with the previous expression found in (3.16)

$$E_{tot} = \frac{GL^5}{90b^6c^5\mu^3}F(\varphi,\varphi_0) \tag{4.20}$$

for different values of ϵ. The system considered here is described by the following set of parameters:

$$m_1 = m_2 = 30M_\odot \tag{4.21}$$
$$v_0 = 0.1c \tag{4.22}$$
$$b = 5...12 \times 10^{-5}AU \tag{4.23}$$

and by varying b we get the following values given in table (4.1).

ϵ	equation (4.32)	equation (4.33)	ΔE
1.31	$6.46 \cdot 10^{43}$J	$6.46 \cdot 10^{43}$J	$< 10^{39}$J
1.42	$2.15 \cdot 10^{43}$J	$2.15 \cdot 10^{43}$J	$< 10^{34}$J
1.68	$4.14 \cdot 10^{42}$J	$4.14 \cdot 10^{42}$J	$< 10^{32}$J
2.26	$5.03 \cdot 10^{41}$J	$5.03 \cdot 10^{41}$J	$< 10^{30}$ J

TABLE 4.1: The total energy for different values of ϵ

*the numerical integration was done over in interval $\nu \in (0, 70)$, see appendix D, note that the numerical accuracy will depend on the interval and integration technique chosen

4.3 Example for an hyperbolic encounter

Consider for example a system of two masses $m_1 = m_2 = 30M_\odot$ with impact velocity $v_0 = 0.1c$ and impact parameter $b = 5 \cdot 10^{-5} AU$ at a distance R from earth of about $0.01Gpc$. The eccentricity for this encounter is roughly given by $\epsilon \approx 1.31$ and therefore $\varphi_0 \approx 2.44$. Using the expressions found in the previous chapters we are able to predict the total released energy, the peak power, the peak frequency and for completeness we also look at the mean strain amplitude observed on earth. The total released energy can be computed with (3.16) and we find for this event $E_{tot} \approx 6.45 \cdot 10^{43} J$. The peak power is given (3.12) and evaluated at φ_0 it is given by $P_{quad}^{max} \approx 2.26 \cdot 10^{41} W$. The peak frequency can be calculated numerically from (4.18) and for this example given by $\omega = 2\pi f \approx 33.88 Hz$.

The strain amplitude h can be found as follows. Using (1.43) we write the mean strain amplitude observed at a distance r as

$$h = \frac{2G}{rc^4} \left\langle \ddot{D}_{ij} \ddot{D}_{ij} \right\rangle^{1/2}. \tag{4.24}$$

The same calculation steps as used in chapter 3 for P_{quad} lead to

$$h(\varphi, \varphi_0) = \frac{2G\mu v_0^2}{rc^4} g(\varphi, \varphi_0), \tag{4.25}$$

with

$$\begin{aligned} g(\varphi, \varphi_0) = 3\csc^4(\varphi_0)(&-20\cos(2(\varphi - \varphi_0)) + 9\cos(\varphi + 2\varphi_0) + 44\cos(\varphi - 2\varphi_0) \\ &-10\cos(2(\varphi - 2\varphi_0)) + 3\cos(3\varphi - 2\varphi_0) + 9\cos(\varphi - 4\varphi_0) + 3\cos(3\varphi - 4\varphi_0) \\ &+44\cos(\varphi) - 10\cos(2\varphi) - 32\cos(2\varphi_0) - 3\cos(4\varphi_0) - 37). \end{aligned} \tag{4.26}$$

The strain amplitude behavior is shown in figure 4.2. Evaluating (4.25) for $\varphi_0 \approx 2.44$ at a distance $R = 0.01Gpc$ we find $h_{max} \approx 6.69 \cdot 10^{-20}$. This signal presented here is in the sensitivity range and frequency band of LIGO [3] . Further interesting examples can be found in the two papers by Garcia-Bellido and Nesseris on gravitational wave bursts from primordial black hole hyperbolic encounters [1, 11] and in the paper by De Vittori et al. [9].

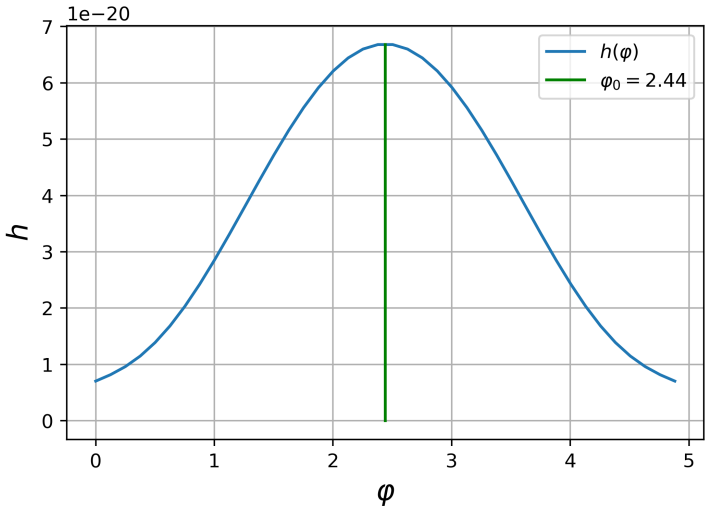

FIGURE 4.2: Strain amplitude for $\epsilon \approx 1.31$

Chapter 5

Eccentricity limits

In this section we will consider the parabolic limit ($\epsilon \to 1$) and qualitatively the limit for large eccentricities ($\epsilon >> 1$).

5.1 Total energy in the parabolic limit $\epsilon \to 1$

We will compare the total energy expressions found here, by Bellido and Nesseris [1] and by Berry and Gair [2] for the case $\epsilon = 1$. The one found here is given by (3.16)

$$E^1_{tot} = \frac{GL^5}{90b^6c^5\mu^3} F(\varphi, \varphi_0) \tag{5.1}$$

with

$$\begin{aligned} F(\varphi, \varphi_0) = \frac{1}{\tan(\varphi_0)^2 \sin(\varphi_0)^4} (2628\varphi_0 + 2328\varphi_0 \cos(2\varphi_0) + 144\varphi_0 \cos(4\varphi_0) \\ -1948 \sin(2\varphi_0) - 301 \sin(4\varphi_0)). \end{aligned} \tag{5.2}$$

The one found by Bellido and Nesseris is given by

$$E^2_{tot} = \frac{8}{15} \frac{G^{7/2}}{c^5} \frac{m^{1/2} m_1^{1/2} m_2^{1/2}}{r_{min}^{7/2}} f(\epsilon), \tag{5.3}$$

with r_{min} is defined by

$$b = r^2_{min} \left(1 + \frac{2Gm}{v_0^2 r_{min}}\right) \tag{5.4}$$

and $f(\epsilon)$ given by

$$f(\epsilon) = \frac{1}{(1+\epsilon)(7/2)} \left[24 \arccos(-1/\epsilon)(1 + \frac{73}{24}\epsilon^2 + \frac{37}{96}) + \sqrt{\epsilon^2 - 1}(\frac{301}{6} + \frac{673}{12}\epsilon^2)\right]. \tag{5.5}$$

The one found by Berry and Gair is given by

$$E^3_{tot} = \frac{64\pi}{5} \frac{G^3}{c^5} \frac{m_1^2 m_2^2}{r_p^2} w_c (1-\epsilon)^{7/2} g(\epsilon), \tag{5.6}$$

with

$$g(\epsilon) = \frac{1 + \frac{73}{24}\epsilon^2 + \frac{37}{96}\epsilon^4}{(1-\epsilon^2)^{7/2}}, \tag{5.7}$$

$$r_p = \frac{1}{2}\frac{L^2}{G\mu^2 m}, \tag{5.8}$$

$$w_c^2 = \frac{G(m_1+m_2)}{r_p^3}. \tag{5.9}$$

In the previous expressions E^1_{tot} and E^2_{tot} are valid for hyperbolic orbits whereas E^3_{tot} is valid for elliptic orbits. To compare all expression we use the following parameters: $v_0 = 0.1c$, $b = 0.1 \cdot 10^{-5} AU$ and $m_1 = m_2 = 30 M_\odot$ which give the eccentricity $\epsilon \approx 1$. Numerical evaluation for all three expression gives $E_{tot} \approx 3.04 \cdot 10^{55} J$.

5.2 Power spectrum in the limit $\epsilon \to 1$

Finding an analytic expression for the limit of the power spectrum 4.18 is rather complicated because if the complexity of the Hankel functions used there. Therefore we will show the qualitative behavior of the power spectrum plot and just give briefly the idea of how we could reach an analytic limit which we could compare with the one found by Berry and Gair [2] . A few power spectra for small values of ϵ are shown in figure 5.1. We see that

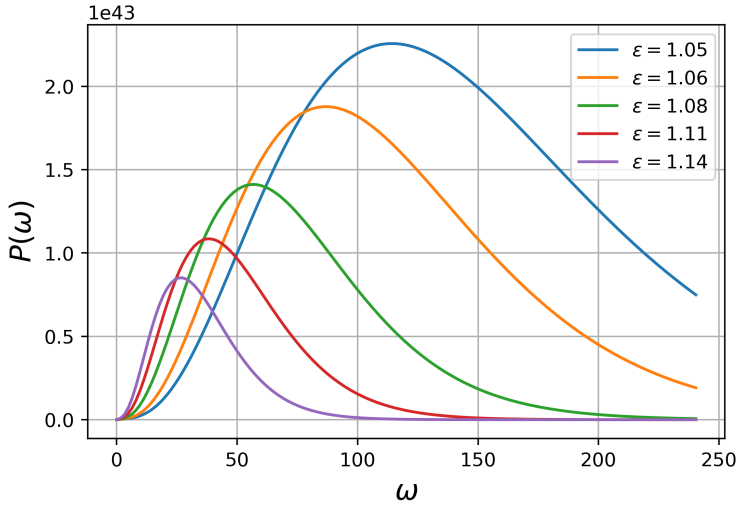

FIGURE 5.1: Power spectrum for small values of ϵ

the peak frequency and the peak power increase with decreasing eccentricity. This is what we would intuitively expect. The closer we are to the parabolic limit the stronger and more violent the gravitational interactions gets and the system releases more and more energy during the encounter.

To find the analytic limit we might start as follows: we know that a parabolic limit is characterized by $\epsilon = 1$, $E = 0$ and $L = const.$ along the orbit. Using the abbreviations from chapter 2 we find the following relations

$$a \sim \frac{1}{E}, \tag{5.10}$$

$$\eta \sim \sqrt{a^3} \sim \frac{1}{E^{3/2}} \tag{5.11}$$

and with this we find

$$\nu \sim \eta \Rightarrow \nu \sim \frac{1}{E^{3/2}}. \tag{5.12}$$

So if we consider the limit $E \to 0$ we have to take the limit $\nu \to \infty$ additionally to $\epsilon \to 1^+$ in (4.18). Taking first the $\epsilon \to 1^+$ limit and ignoring the prefactor for a moment we get

$$P(\omega) \sim \nu^4 \frac{6}{\nu^2} \left| H_{i\nu}^{(1)}(i\nu\epsilon) \right|^2. \tag{5.13}$$

The most general expansion for the Hankel function is given by (9.3.37) in Abramowitz and Stegun [13] as follows

$$\begin{aligned} H_\nu^{(1)}(\nu z) \sim 2e^{-\pi i/3} \left(\frac{4\zeta}{1-z^2} \right)^{1/4} \{ & \frac{\mathrm{Ai}(e^{(2\pi i/3)}\nu^{2/3}\zeta)}{\nu^{1/3}} \sum_{k=0}^{\infty} \frac{a_k(\zeta)}{\nu^{2k}} + \\ & \frac{\mathrm{Ai}'(e^{(2\pi i/3)}\nu^{2/3}\zeta)}{\nu^{5/3}} \sum_{k=0}^{\infty} \frac{b_k(\zeta)}{\nu^{2k}} \}. \end{aligned} \tag{5.14}$$

To use this expansion for our problem we have to substitute $\nu \to i\nu$ and $z \to \epsilon$. To proceed further we need to expand each part in (5.14) very carefully for our limits. This is a rather difficult mathematical problem and during this work we could not find a satisfying solution.Garcia-Bellido and Nesseris used in their most recent paper [1] equations (9.3.15 - 9.3.20) of Abramowitz and Stegun. But this ansatz might be wrong since these expansions are bound to certain conditions regarding the parameter values which are in general violated for our case here. An analytic solution for the parabolic limit starting from elliptic orbits and taking $\epsilon \to 1^-$ was found by Berry and Gair [2]. Their result might help to find the limit considered here since both approaches should coincide in the parabolic limit. In the paper by De Vittori, Jetzer and Klein [9] they already started a discussion about this limit but unfortunately with the wrong expression for the power spectrum in hand. Maybe with the correct result their argumentation might lead in the right direction.

5.3 Power spectrum in the limit $\epsilon >> 1$

A few power spectra for larger eccentricities are shown in figure 5.2 below. We see that for

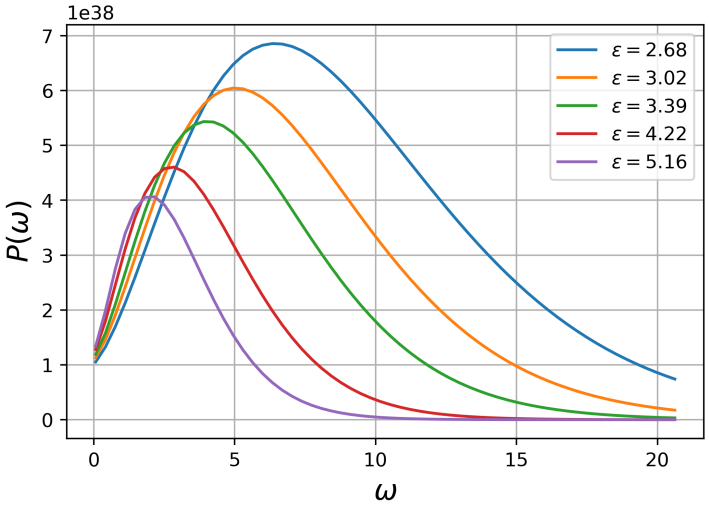

FIGURE 5.2: Power spectrum for greater values of ϵ

increasing eccentricity the peak frequency and peak power decrease. That is also what we would expect, since for a weaker interaction less energy is released during the encounter.

Chapter 6

Back-reaction effects

In this section we will briefly look at some back reaction effects on different quantities of the system.

6.1 Changes in the eccentricity ϵ

ϵ is given by

$$\epsilon = \sqrt{1 + \frac{2EL^2}{\mu\alpha^2}} = \sqrt{1 + KEL^2}, \tag{6.1}$$

where $K = \frac{2}{\mu\alpha^2}$. The change over time of ϵ is given by

$$\begin{aligned} \frac{d\epsilon}{dt} &= \frac{\partial\epsilon}{\partial E}\frac{dE}{dt} + \frac{\partial\epsilon}{\partial L}\frac{dL}{dt} \\ &= \frac{KL^2}{2\epsilon}\frac{dE}{dt} + \frac{KEL}{\epsilon}\frac{dL}{dt}. \end{aligned} \tag{6.2}$$

To lowest order we can assume that both prefactors, $\frac{KL^2}{2\epsilon}$ and $\frac{KEL}{\epsilon}$, are constants. Following the post-Newtonian procedure we can approximate each quantity in a series like $E \approx E_0 + E^{(1)} + E^{(2)} + \ldots$ and $L \approx L_0 + L^{(1)} + L^{(2)} + \ldots$. Since $\frac{dE}{dt}$ and $\frac{dL}{dt}$ are already first order terms we can ignore all higher order terms in the expansions except for the lowest order which we will set to $E \equiv E_0$ and $L \equiv L_0$. By doing so we get the change in ϵ to first order. $\frac{dE}{dt}$ is already given in (3.12) and using $P = -\frac{dE}{dt}$ we are left with finding an equivalent expression for $\frac{dL}{dt}$. In Maggiore's book [7] the general expression for $\frac{dL}{dt}$ in the quadrupole approximation is given by

$$\frac{dL^i}{dt} = -\frac{2G}{5c^5}\epsilon^{ikl}\langle \ddot{M}_{ka}\dddot{M}_{la}\rangle. \tag{6.3}$$

Since the motion is restricted to the x-y-plane we look at the change of $L^z \equiv L$, corresponding to $i = 3$. Using the symmetry of the mass moment $M_{ab} = M_{ba}$ and the permutation properties of the Levi-Civita-Symbol ϵ^{ikl} we find

$$\frac{dL}{dt} = -\frac{2G}{5c^5}\left(\ddot{M}_{12}(\dddot{M}_{22} - \dddot{M}_{11}) + \dddot{M}_{12}(\ddot{M}_{11} - \ddot{M}_{22})\right). \tag{6.4}$$

Here we use again the following expressions for the mass momenta

$$M_{11} = \mu r(\varphi)^2 \cos^2(\varphi), \tag{6.5}$$
$$M_{11} = \mu r(\varphi)^2 \sin^2(\varphi), \tag{6.6}$$
$$M_{12} = M_{21} = \mu r(\varphi)^2 \cos(\varphi)\sin(\varphi), \tag{6.7}$$
$$\tag{6.8}$$

with

$$r(\varphi) = \frac{b\sin(\varphi_0)}{\cos(\varphi-\varphi_0)-\cos(\varphi_0)} \tag{6.9}$$

and

$$\frac{d\varphi}{dt} = \frac{L}{\mu r(\varphi)^2}. \tag{6.10}$$

Following the same steps as we did for $\frac{dE}{dt}$ we get

$$\frac{dL}{dt} = -\frac{16}{5}\frac{GL^5}{c^5\mu^3 b^6}\tilde{f}(\varphi,\varphi_0), \tag{6.11}$$

with

$$\begin{aligned}\tilde{f}(\varphi,\varphi_0) = \frac{\sin(\frac{\varphi}{2})^3\sin(\frac{1}{2}(\varphi-2\varphi_0))^3}{\sin(\varphi_0)^6}[-6\cos(\varphi-3\varphi_0)+3\cos(2\varphi-3\varphi_0)\\ -12\cos(\varphi-\varphi_0)+3\cos(2\varphi-\varphi_0)+14\cos(\varphi_0)+4\cos(3\varphi_0)-6\cos(\varphi+\varphi_0)].\end{aligned} \tag{6.12}$$

For completeness $\frac{dE}{dt}$ is given by

$$\frac{dE}{dt} = -P_{quad}(\varphi) = -\frac{32GL^6}{45c^5b^8\mu^4}f(\varphi,\varphi_0), \tag{6.13}$$

with

$$\begin{aligned}f(\varphi,\varphi_0) = \frac{\sin(\frac{\varphi}{2}-\varphi_0)^4\sin(\frac{\varphi}{2})^4}{\tan(\varphi_0)^2\sin(\varphi_0)^6}[150+72\cos(2\varphi_0)+66cos(2\varphi_0-2\varphi)\\ -144(\cos(\varphi-2\varphi_0)+\cos(\varphi))].\end{aligned} \tag{6.14}$$

Inserting the expressions for $\frac{dE}{dt}$ and $\frac{dL}{dt}$ in (6.2) we get

$$\frac{d\epsilon}{dt} = -\frac{16}{45}\frac{KGL^8}{c^5b^8\mu^4\epsilon}f(\varphi,\varphi_0) - \frac{16}{5}\frac{KGL^6E}{c^5\mu^3b^6\epsilon}\tilde{f}(\varphi,\varphi_0). \tag{6.15}$$

In order to find the total change of ϵ during the encounter we have to integrate the expression over the whole trajectory, meaning from $\varphi = 0$ to $\varphi = 2\varphi_0$. Therefore we switch from dt to $d\varphi$ on the right hand side in (6.15) using (6.10). Our final expression, which is left to integrate is then given by

$$\frac{d\epsilon}{d\varphi} = \frac{\mu r(\varphi,\varphi_0)^2}{L}\left(-\frac{16}{45}\frac{KGL^8}{c^5b^8\mu^4\epsilon}f(\varphi,\varphi_0) - \frac{16}{5}\frac{KGL^6E}{c^5\mu^3b^6\epsilon}\tilde{f}(\varphi,\varphi_0)\right). \tag{6.16}$$

Integration over φ gives

$$\begin{aligned} F(b,\varphi_0) &= \int_0^{2\varphi_0} r(\varphi,\varphi_0)^2 f(\varphi,\varphi_0) d\varphi \\ &= \frac{1}{128} b^2 \frac{(2628\varphi_0 - 1948\sin(2\varphi_0) - 301\sin(4\varphi_0) + 2328\varphi_0\cos(2\varphi_0) + 144\varphi_0\cos(4\varphi_0))}{\tan^2(\varphi_0)\sin^4(\varphi_0)} \end{aligned} \tag{6.17}$$

and

$$\begin{aligned} \tilde{F}(b,\varphi_0) &= \int_0^{2\varphi_0} r(\varphi,\varphi_0)^2 \tilde{f}(\varphi,\varphi_0) d\varphi \\ &= \frac{1}{16} b^2 \frac{(-21\sin(\varphi_0) - 13\sin(3\varphi_0) + 52\varphi_0\cos(\varphi_0) + 8\varphi_0\cos(3\varphi_0))}{\tan(\varphi_0)\sin^3(\varphi_0)}. \end{aligned} \tag{6.18}$$

Finally, the total change in the eccentricity $\Delta\epsilon$ can be written as

$$\Delta\epsilon = -\frac{16}{45}\frac{KGL^7}{c^5 b^8 \mu^3 \epsilon} F(b,\varphi_0) - \frac{16}{5}\frac{KGL^5 E}{c^5 \mu^2 b^6 \epsilon}\tilde{F}(b,\varphi_0). \tag{6.19}$$

Using $L = \mu b v_0$, $E = \frac{1}{2}\mu v_0^2$, $K = \frac{2}{\mu\alpha^2}$ and $\alpha = Gm\mu$ we can rewrite the prefactors as follows

$$\frac{KGL^7}{c^5 b^8 \mu^3 \epsilon} = \frac{2G\mu^7 b^7 v_0^7}{\mu^3 G^2 m^2 c^5 b^8 \mu^3 \epsilon} = \frac{2\mu v_0^7}{Gb\epsilon m^2 c^5}, \tag{6.20}$$

$$\frac{KGL^5 E}{c^5 \mu^2 b^6 \epsilon} = \frac{2G\mu^5 b^5 v_0^5 \mu v_0^5}{2\mu^3 G^2 m^2 c^5 \mu^2 b^6 \epsilon} = \frac{\mu v_0^7}{Gb\epsilon m^2 c^5}, \tag{6.21}$$

which gives

$$\Delta\epsilon = \epsilon_{end} - \epsilon_{begin} = -\frac{\mu v_0^7}{Gb\epsilon m^2 c^5}\left(\frac{32}{45}F(b,\varphi_0) + \frac{16}{5}\tilde{F}(b,\varphi_0)\right). \tag{6.22}$$

So after the encounter we find the following eccentricity

$$\epsilon_{end} = \Delta\epsilon + \epsilon_{begin}. \tag{6.23}$$

The total change $\Delta\epsilon$ as given in equation (6.22) is a function of the impact parameter b, total mass $m = m_1 + m_2$ and impact velocity v_0. Remember that for a hyperbolic trajectory we can write ϵ as a function of those parameters as

$$\epsilon = \epsilon(v_0, b, m) = \sqrt{1 + \frac{v_0^4 b^2}{G^2 m^2}}. \tag{6.24}$$

In order to get a qualitative overview of the behavior of ϵ_{end} as a function of b, m and v_0 we set two parameters equal to a fixed value and vary the third one. The results are plotted in figure 6.1, 6.2 and 6.3. Since the system will lose energy and angular momentum during the encounter eccentricity will decrease and can become smaller than 1 under certain conditions. The following plots show the behavior around these critical parameters. We denote the parameter value for which $\epsilon_{end} = 1$ as critical value with the subscript "crit". While considering the plots it is also important to keep in mind that we work in the regime of a hyperbolic encounter so the functional behavior will be valid only up to $\epsilon_{end} = 1$ and below one has to consider the equations valid for elliptic trajectories. See for example the work

done by Blanchet and Schäfer [9], who extended the work done by Peter and Mathews [8] to describe capture processes. The valid region is therefore marked in all plots explicitly. One can test for different sets of parameters and find different sets of critical values. But in general one finds values for the critical eccentricity around 1.05, so already close to the limiting case $\epsilon_{begin} = 1$. This means that the initial parameters have to be close the parabolic case $\epsilon = 1$ in order to be captured from a hyperbolic orbit into a bound orbit as a result of the back-reaction effect from the emission of gravitational waves.

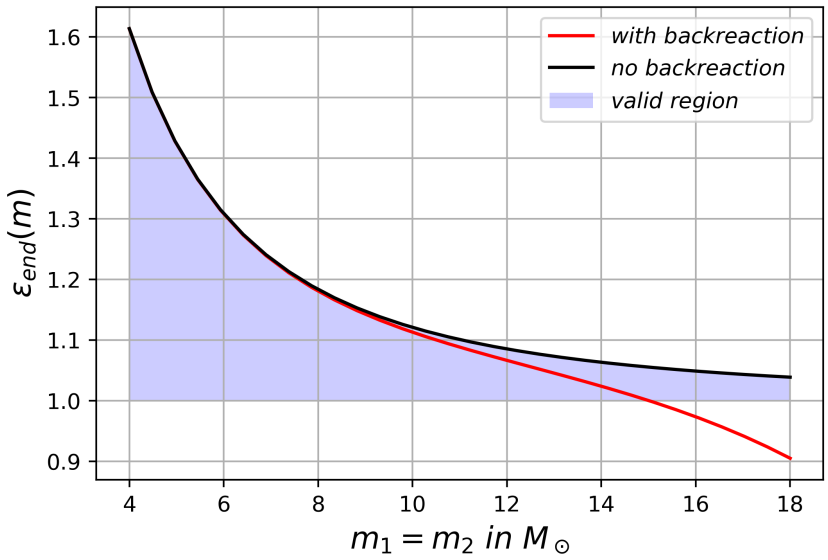

FIGURE 6.1: We fix $b = 10^{-5} AU$ and $v_0 = 0.1c$ and vary $m_1 = m_2$ in the interval $4M_\odot - 18M_\odot$. The critical mass is given by $m_{crit} \approx 15.1M_\odot$ with corresponding critical value for the initial eccentricity of $\epsilon_{crit} \approx 1.055$.

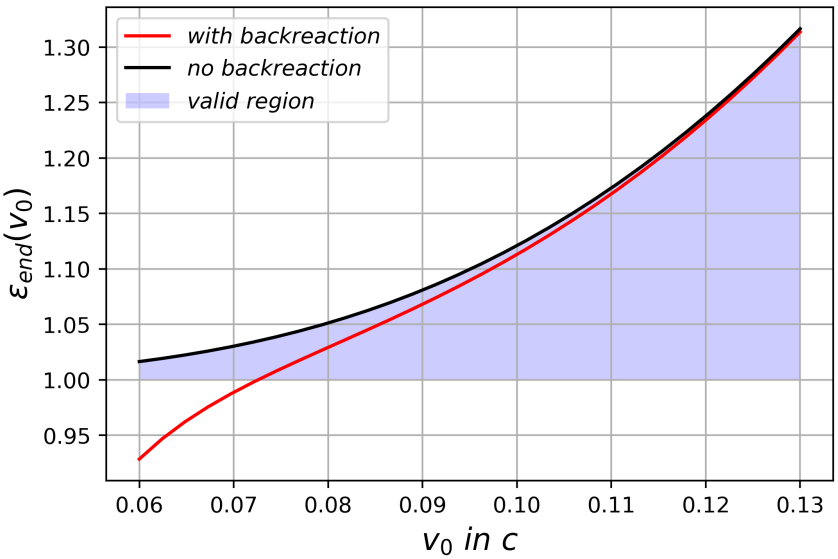

FIGURE 6.2: We fix $b = 10^{-5}AU$ and $m_1 = m_2 = 10M_\odot$ and vary v_0 in the interval $0.06c - 0.13c$. The critical velocity is given by $v_{crit} \approx 0.72c$ with corresponding critical value for the initial eccentricity of $\epsilon_{crit} \approx 1.034$.

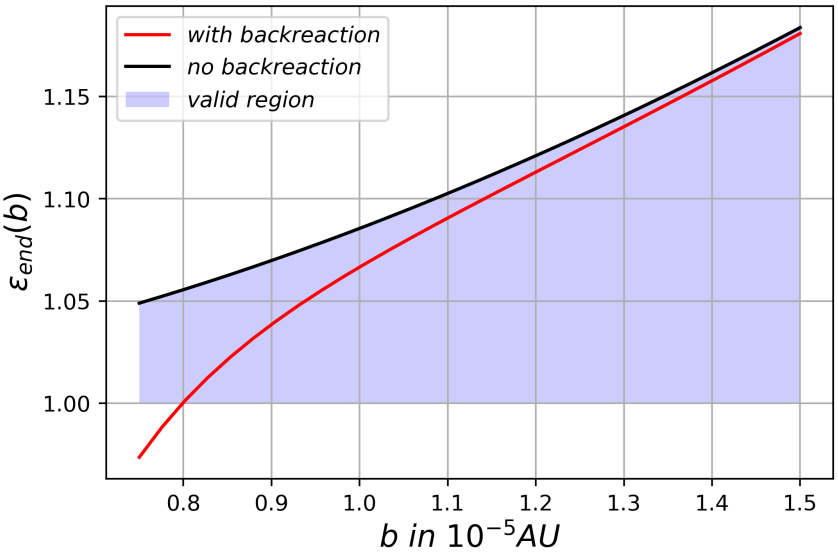

FIGURE 6.3: We fix $v_0 = 0.1c$ and $m_1 = m_2 = 12M_\odot$ and vary b in the interval $0.75 \cdot 10^{-5}AU - 1.2 \cdot 10^{-5}AU$. The critical impact parameter is given by $b_{crit} \approx 0.8 \cdot 10^{-5}AU$ with corresponding critical value for the initial eccentricity of $\epsilon_{crit} \approx 1.054$.

Chapter 7

Discussion

The basic idea of this thesis was to revisit the paper written by De Vittori, Jetzer and Klein [9] and find the correct expression for the gravitational wave power spectrum of hyperbolic encounters, since the original paper had inconsistencies in the corresponding expression. When we started this work we didn't know yet that Garcia-Bellido and Nesseris worked on this problem and after they published their paper in November 2017 we compared the results found here with their result and found an agreement. The calculated power along the orbit and power spectrum as plotted in figure 3.2 and 4.1, respectively, show the behavior we expect from a hyperbolic encounter. The power increases along the orbit until the closet approach, point of strongest gravitational interaction, is reached and then decreases again. The same behavior is also shown by the strain amplitude as shown in figure 4.2. So the emission is a gravitational wave burst with a peak at the closet approach. The strength of the burst is very sensitive to all impact parameters and masses in the system. The eccentricity for the hyperbolic encounter is given in 2.11 and we can reach the same eccentricity with different sets of parameters. Since the strength of the emitted energy, power and strain amplitude is determined by their prefactors, as seen in equation (3.12), (3.16) and (4.25), the impact parameters determine their magnitude. If we vary the impact parameters we see that for high velocities, big masses and small impact parameter we get a large energy and power release and a large strain amplitude. Assuming the opposite case of impact parameters we get a small energy and power release and a small strain amplitude signal. An interesting example in the context of primordial Black Holes can be found in the papers [1, 11] by Garcia-Bellido and Nesseris. It is nevertheless important to keep in mind that we worked in quadrupole approximation and used Newton's equation to describe the hyperbolic trajectory. If the system velocity become larger the higher order terms in $\frac{v}{c}$ become more important and we have to go beyond the lowest order quadrupole formulation. Equivalently if the masses become larger and the impact parameter smaller we have to add corrections to the Newtonian equations describing the trajectory. This could be done by adding post-Newtonian terms. But if we want to detect hyperbolic encounters we rely on large system parameters and a violent interaction, such that the signal is strong enough to be detected by any gravitational wave detector. In chapter 6 we were also able to show that for a critical set of impact parameters we lose enough energy through gravitational wave emission such that the back-reaction effect leads to a capture process, meaning that the eccentricity decreases below 1. In figure 6.3 - 6.3 we could show, using equation (6.23), that if the masses are large enough, the velocity is low enough or the impact parameter is small enough that the hyperbolic trajectory turns into a bound orbit. The critical parameters which lead to the process will depend on the full set of initial parameters. A consistency check of our results was done by comparison with older works on gravitational wave emission from elliptic orbits by considering the parabolic limit. We did a numerical comparison between our results and the one given by Berry and Gair [2] and found a complete agreement despite the different approaches taken. What is still an open problem, is to find an analytic agreement between the power spectrum as given here and the one given by Berry and Gair. But this is more a mathematical problem rather

than one of physical understanding.

Chapter 8

Conclusion

The thesis written here was guided and inspired by older works and some more recent works on gravitational wave emission. These were the papers on elliptic orbits by Peter and Mathews [8] , Berry and Gair [2] , Blanchet and Schäfer [10] and the works on hyperbolic orbits by, Vittori, Jetzer and Klein [9] , Capozziello et. al. [6] , Turner [14] and Garcia-Bellido and Nesseris [1] . This thesis can be seen as a summary and extension of previous works and will be useful for studying the topic of gravitational wave emission from hyperbolic orbits. All important expressions found here show an agreement with our qualitative expectations and the numerical evaluations show that it will be possible for LISA and LIGO to detect such events in the future. The found power spectrum and strain amplitude might be useful to design future detectors for the detection of such gravitational wave bursts, see for example [1].

Bibliography

[1] Juan Garcia-Bellido and Savvas Nesseris,"Gravitational wave energy emission and detection rates of Primordial Black Hole hyperbolic encounters", November 2017, arXiv:1711.09702

[2] Christopher P. L. Berry and Jonathan R. Gair, "Gravitational wave energy spectrum of a parabolic encounter",Phys.Rev.D82:107501 (2010) ,arXiv:1010.3865

[3] "The Sensitivity of the Advanced LIGO Detectors at the Beginning of Gravitational Wave Astronomy ", Phys. Rev. D 93, 112004 (2016), arXiv:1604.00439

[4] LIGO Scientific Collaboration and Virgo Collaboration,"Observation of Gravitational Waves from a Binary Black Hole Merger",Phys. Rev. Lett. 116,061102 (2016)

[5] LIGO Scientific Collaboration and Virgo Collaboration,"GW170817: Observation of Gravitational Waves from a Binary Neutron Star Inspiral", Phys. Rev. Lett. 119, 161101 (2017)

[6] S. Capozziello and M. De Laurentis and F.De Paolis and G. Ingrosso and A. Nucita,"Gravitational waves from hyperbolic encounters",Mod.Phys.Lett.A23:99-107 (2008), arXiv:0801.0122

[7] Michele Maggiore, "Gravitational Waves Volume 1: Theory and Experiments", Oxford University Press

[8] P.C. Peters and J. Mathews,"Gravitational Radiation from Point Masses in a Keplerian Orbit", Phys. Rev. 131, 435

[9] Lorenzo De Vittori, Philippe Jetzer, Antoine Klein,"Gravitational wave energy spectrum of hyperbolic encounters",Phys.Rev.D 86 (2012) 044017, arXiv:1207.5359

[10] L.Blanchet and G. Schäfer,"Higher order gravitational radiation losses in binary systems", Monthly Notices of the Royal Astronomical Society (ISSN 0035-8711), vol. 239, Aug. 15, 1989, p. 845-867

[11] Juan Garcia-Bellido and Savvas Nesseris,"Gravitational wave bursts from Primordial Black Hole hyperbolic encounters",Phys.Dark Univ., 18 (2017) 123-126, arXiv:1706.02111

[12] L.D.Landau and E.M.Lifshitz,"The Classical Theory of Fields" Volume 2

[13] M.Abramowitz and I.A.Stegun,"Handbook of mathematical functions",see also the Digital Library of Mathematical Functions (dlmf)

[14] M. Turner,"Gravitational radiation from point-masses in unbound orbits - Newtonian results", Astrophysical Journal, Part 1, vol. 216, Sept. 1, 1977, p. 610-619, http://adsabs.harvard.edu/full/1977ApJ...216..610T

Appendix A

Fourier transformation

A.1 Time derivative

$$\hat{f}(\omega) = \int_{\mathbb{R}} f(t) e^{i\omega t} dt \tag{A.1}$$

$$\hat{\dot{f}}(\omega) = \int_{\mathbb{R}} \dot{f}(t) e^{i\omega t} dt \tag{A.2}$$

$$= f(t) e^{i\omega t}|_{\mathbb{R}} - \int_{\mathbb{R}} f(t)(i\omega) e^{i\omega t} dt \tag{A.3}$$

$$\tag{A.4}$$

For physical functions the first term is bound therefore will vanishes and we are left with

$$\hat{\dot{f}}(\omega) = -i\omega \hat{f}(\omega). \tag{A.5}$$

Iteration gives the general rule

$$\hat{f^{(n)}}(\omega) = (-i\omega)^n \hat{f}(\omega). \tag{A.6}$$

A.2 Parseval identity

Proof:

$$\begin{aligned}
\int_{-\infty}^{+\infty} |f(t)|^2 dt &= \int_{-\infty}^{+\infty} f(t) f(t)^* dt \\
&= \int_{-\infty}^{+\infty} \left(\frac{1}{2\pi} \int_{\mathbb{R}} \hat{f}(\omega) e^{-i\omega t} d\omega \right) \left(\frac{1}{2\pi} \int_{\mathbb{R}} \hat{f}(\omega') e^{-i\omega' t} d\omega' \right)^* dt \\
&= \frac{1}{(2\pi)^2} \int_{-\infty}^{+\infty} \int_{\mathbb{R}} \int_{\mathbb{R}} \hat{f}(\omega) \hat{f}(\omega')^* e^{-i(\omega-\omega')t} d\omega d\omega' dt \\
&\overset{(4.3)}{=} \frac{1}{2\pi} \int_{\mathbb{R}} \hat{f}(\omega) \hat{f}(\omega)^* d\omega \\
&\underbrace{=}_{\text{symmetry}} \int_0^{+\infty} \frac{|\hat{f}(\omega)|^2}{\pi} d\omega,
\end{aligned} \tag{A.7}$$

with * denoting the complex conjugate.

Appendix B

Inavariance of mass quadrupole moment

Consider the following mass quadrupole moment

$$M^{ij} = \frac{1}{c^2}\int d^3x T^{00}(t,\vec{c})x^i x^j \tag{B.1}$$

for a system of non-relativistic particles with

$$T^{00}(t,\vec{x}) = \sum_k m_k c^2 \delta^3(\vec{x}-\vec{x}_k). \tag{B.2}$$

Using T^{00} we can write

$$M^{ij} = \sum_k m_k x_k^i x_k^j. \tag{B.3}$$

Now we perform a constant coordinate shift (shift of the origin) of the following form

$$x^i \to x^i + a^i, \tag{B.4}$$

which leads to

$$\begin{aligned} M^{ij} \to \tilde{M}^{ij} &= \sum_k m_k (x_k^i + a^i)(x_k^j + a^j) \\ &= \sum_k m_k x_k^i x_k^j + \sum_k m_k x_k^i a^j + \sum_k m_k a^i x_k^j + \sum_k m_k a^i a^j. \end{aligned} \tag{B.5}$$

Performing a time derivative and define $P^i_{tot} = \sum_k P^i_k$ we get

$$\dot{\tilde{M}}^{ij} = \dot{M}^{ij} + a^i P^i_{tot} + a^j P^j_{tot}. \tag{B.6}$$

Since we consider a closed system $P^i_{tot} = const$ and higher order time derivatives (∂_t^2 and higher) will give

$$\ddot{\tilde{M}}^{ij} = \ddot{M}^{ij} \tag{B.7}$$

and therefore the third time derivative of any quadrupole mass moment will be invariant under constant coordinate shift.

Appendix C

Fourier transformation used for the power spectrum

C.1 Fourier transformation of *sinh* and *cosh*

Useful relations:

$$t(\xi) = \eta(\epsilon \sinh(\xi) - \xi) \tag{C.1}$$

$$\frac{dt}{d\xi} = \eta(\epsilon \cosh(\xi) - 1) \tag{C.2}$$

$$\sinh(n\xi) = \frac{1}{2}(e^{n\xi} - e^{-n\xi}) \tag{C.3}$$

$$\cosh(n\xi) = \frac{1}{2}(e^{n\xi} + e^{-n\xi}). \tag{C.4}$$

From Landau-Lifshitz [12] Eq. (70.17)

$$H_p^{(1)}(ix) = \frac{1}{i\pi} \int_{\mathbb{R}} e^{ix \sinh(\xi) - p\xi} d\xi. \tag{C.5}$$

For $\sinh(n\xi)$ we get

$$\widehat{sinh}(n\xi) = \int_{\mathbb{R}} \sinh(n\xi) e^{i\omega t(\xi)} dt \tag{C.6}$$

$$= \int_{\mathbb{R}} \sinh(n\xi) e^{i\omega t(\xi)} \frac{dt}{d\xi} d\xi \tag{C.7}$$

$$= \eta \int_{\mathbb{R}} \sinh(n\xi) e^{i\omega\eta(\epsilon \sinh(\xi) - \xi)} (\epsilon \cosh(\xi) - 1) dt \tag{C.8}$$

$$= \frac{\eta\epsilon}{4} \int_{\mathbb{R}} (e^{n\xi} - e^{-n\xi})(e^{\xi} + e^{-\xi}) e^{i\omega\eta(\epsilon \sinh(\xi) - \xi)} d\xi$$

$$- \frac{\eta}{2} \int_{\mathbb{R}} (e^{n\xi} - e^{-n\xi}) e^{i\omega\eta(\epsilon \sinh(\xi) - \xi)} d\xi \tag{C.9}$$

$$= \frac{\eta\epsilon}{4} \int_{\mathbb{R}} e^{i\omega\eta\epsilon \sinh(\xi) + (n+1-i\omega\eta)\xi} - e^{i\omega\eta\epsilon \sinh(\xi) + (-n+1-i\omega\eta)\xi}$$

$$+ e^{i\omega\eta\epsilon \sinh(\xi) + (n-1-i\omega\eta)\xi} - e^{i\omega\eta\epsilon \sinh(\xi) + (-n-1-i\omega\eta)\xi} d\xi$$

$$- \frac{\eta}{2} \int_{\mathbb{R}} e^{i\omega\eta\epsilon \sinh(\xi) + (n-i\omega\eta)\xi} - e^{i\omega\eta\epsilon \sinh(\xi) + (-n-i\omega\eta)\xi} d\xi \tag{C.10}$$

Defining $z = i\omega\eta\epsilon$ and using (C.5) we get

$$\begin{aligned}\widehat{sinh}(n\xi) = \frac{i\pi\eta\epsilon}{4}[H^{(1)}_{(-n-1+i\omega\eta)}(z) - H^{(1)}_{(n-1+i\omega\eta)}(z) + H^{(1)}_{(-n+1+i\omega\eta)}(z) \\ + H^{(1)}_{(n+1+i\omega\eta)}(z)] - \frac{i\pi\eta}{2}[H^{(1)}_{(-n+i\omega\eta)}(z) - H^{(1)}_{(n+i\omega\eta)}(z)].\end{aligned} \tag{C.11}$$

Now we use

$$z = i\omega\eta\epsilon \tag{C.12}$$

$$\frac{2\alpha}{z}H^{(1)}_{\alpha}(z) = H^{(1)}_{\alpha-1}(z) + H^{(1)}_{\alpha+1}(z) \tag{C.13}$$

to get

$$\begin{aligned}\widehat{sinh}(n\xi) &= \frac{i\pi\eta\epsilon}{4}\frac{2(i\omega\eta - n)}{2}H^{(1)}_{(i\omega\eta-n)}(z) - \frac{i\pi\eta\epsilon}{4}\frac{2(i\omega\eta + n)}{2}H^{(1)}_{(i\omega\eta+n)}(z) \\ &\quad - \frac{\eta i\pi}{2}H^{(1)}_{(i\omega\eta-n)}(z) + \frac{\eta i\pi}{2}H^{(1)}_{(i\omega\eta+n)}(z) \qquad \text{(C.14)} \\ &= \left(\frac{i\pi\eta\epsilon(i\omega\eta - n)}{2i\omega\eta\epsilon} - \frac{\eta i\pi}{2}\right)H^{(1)}_{(i\omega\eta-n)}(z) \\ &\quad + \left(-\frac{i\pi\eta\epsilon(i\omega\eta + n)}{2i\omega\eta\epsilon} + \frac{\eta i\pi}{2}\right)H^{(1)}_{(i\omega\eta+n)}(z) \qquad \text{(C.15)} \\ &= -\frac{\pi n}{2\omega}\left(H^{(1)}_{(i\omega\eta+n)}(z) + H^{(1)}_{(i\omega\eta-n)}(z)\right). \qquad \text{(C.16)}\end{aligned}$$

The calculation for $\widehat{cosh}(n\xi)$ is equivalent, except for a sign change and will lead to

$$\widehat{cosh}(n\xi) = -\frac{\pi n}{2\omega}\left(H^{(1)}_{(i\omega\eta-n)}(z) - H^{(1)}_{(i\omega\eta+n)}(z)\right). \tag{C.17}$$

So we finally have:

$$\widehat{sinh}(n\xi) = -\frac{\pi n}{2\omega}\left(H^{(1)}_{(i\omega\eta+n)}(z) + H^{(1)}_{(i\omega\eta-n)}(z)\right) \tag{C.18}$$

$$\widehat{cosh}(n\xi) = -\frac{\pi n}{2\omega}\left(H^{(1)}_{(i\omega\eta-n)}(z) - H^{(1)}_{(i\omega\eta+n)}(z)\right). \tag{C.19}$$

For comparison with Bellido and Nesseris [1] the following relations hold $\eta = v_0$, $\nu = \omega v_0 = \omega\eta$ and $e = \epsilon$.

C.2 Fourier transformation of the momenta D_{ij}

We are using the expressions given in chapter 4 and ignore all constant prefactors here for simplicity. We use the following notations:

$$\nu = \omega\eta \tag{C.20}$$

$$z = i\omega\eta\epsilon = i\nu\epsilon \tag{C.21}$$

and the following identities,see Abramowitz [13] , for the Hankel functions:

$$H^{(1)}_{\alpha-1}(z) + H^{(1)}_{\alpha+1}(z) = \frac{2\alpha}{z} H^{(1)}_{\alpha}(z) \tag{C.22}$$

$$H^{(1)}_{\alpha-1}(z) - H^{(1)}_{\alpha+1}(z) = 2H^{(1)\prime}_{\alpha}(z) \tag{C.23}$$

$$H^{(1)}_{\alpha-2}(z) + H^{(1)}_{\alpha+2}(z) = \left(\frac{4\alpha^2}{z^2} - 2\right) H^{(1)}_{\alpha}(z) - \frac{4}{z} H^{(1)\prime}_{\alpha}(z) \tag{C.24}$$

$$H^{(1)}_{\alpha-2}(z) - H^{(1)}_{\alpha+2}(z) = \frac{4\alpha^2}{z} H^{(1)\prime}_{\alpha}(z) - \frac{4\alpha}{z^2} H^{(1)}_{\alpha}(z). \tag{C.25}$$

For the momenta we get the following expressions:

$$\begin{aligned}
\widehat{D_{11}} &= (3-\epsilon^2)\widehat{\cosh}(2\xi) - 8\epsilon\widehat{\cosh}(\xi) \\
&= -(3-\epsilon^2)\frac{\pi}{\omega}[H^{(1)}_{i\nu-2}(z) - H^{(1)}_{i\nu+2}(z)] + \frac{4\pi\epsilon}{\omega}[H^{(1)}_{i\nu-1}(z) - H^{(1)}_{i\nu+1}(z)] \\
&= -(3-\epsilon^2)\frac{\pi}{\omega}[\frac{4i\nu}{z} H^{(1)\prime}_{i\nu}(z) - \frac{4i\nu}{z^2} H^{(1)}_{i\nu}(z)] + \frac{4\pi\epsilon}{\omega} 2H^{(1)\prime}_{i\nu}(z) \\
&= \left[\frac{8\pi\epsilon}{\omega} - \frac{4(3-\epsilon)\pi i\omega\eta}{i\omega^2\eta\epsilon}\right] H^{(1)\prime}_{i\nu}(z) + \frac{4(3-\epsilon^2)i\omega\eta\pi}{-\omega^3\eta^2\epsilon^2} H^{(1)}_{i\nu}(z) \\
&= 4\pi\frac{3(\epsilon^2-1)}{\epsilon}\frac{\eta}{\nu} H^{(1)\prime}_{i\nu}(z) - 4\pi\frac{(3-\epsilon^2)}{\epsilon^2}\frac{i}{\nu}\frac{\eta}{\nu} H^{(1)}_{i\nu}(z) \\
&= 4\pi\frac{\eta}{\nu}\left(\frac{3(\epsilon^2-1)}{\epsilon} H^{(1)\prime}_{i\nu}(z) - \frac{(3-\epsilon^2)}{\epsilon^2}\frac{i}{\nu} H^{(1)}_{i\nu}(z)\right)
\end{aligned} \tag{C.26}$$

$$\begin{aligned}
\widehat{D_{22}} &= 4\epsilon\widehat{\cosh}(\xi) - 3\widehat{\cosh}(2\xi) + 2\epsilon^2\widehat{\cosh}(2\xi) \\
&= -\frac{4\epsilon\pi}{2\omega}[H^{(1)}_{i\nu-1}(z) - H^{(1)}_{i\nu+1}(z)] + \frac{3\pi}{\omega}[H^{(1)}_{i\nu-2}(z) - H^{(1)}_{i\nu+2}(z)] - \frac{2\epsilon^2\pi}{\omega}[H^{(1)}_{i\nu-2}(z) - H^{(1)}_{i\nu+2}(z)] \\
&= -\frac{4\epsilon\pi}{2\omega} 2H^{(1)\prime}_{i\nu}(z) + \frac{3\pi}{\omega}[\frac{4i\nu}{z} H^{(1)\prime}_{i\nu}(z) - \frac{4i\nu}{z^2} H^{(1)}_{i\nu}(z)] - \frac{2\epsilon^2\pi}{\omega}[\frac{4i\nu}{z} H^{(1)\prime}_{i\nu}(z) - \frac{4i\nu}{z^2} H^{(1)}_{i\nu}(z)] \\
&= \left(-\frac{4\epsilon\pi}{\omega} + \frac{3\pi}{\omega}\frac{4i\nu}{z} - \frac{2\epsilon^2\pi}{\omega}\frac{4i\nu}{z}\right) H^{(1)\prime}_{i\nu}(z) + \left(-\frac{3\pi}{\omega}\frac{4i\nu}{z^2} + \frac{2\epsilon^2\pi}{\omega}\frac{4i\nu}{z^2}\right) H^{(1)}_{i\nu}(z) \\
&= 12\pi\frac{(1-\epsilon^2)}{\epsilon}\frac{\eta}{\nu} H^{(1)\prime}_{i\nu}(z) + 4\pi\frac{(-2\epsilon^2+3)}{\epsilon}\frac{i}{\nu}\frac{\eta}{\nu} H^{(1)}_{i\nu}(z) \\
&= \frac{4\pi\eta}{\nu}\left[\frac{3(1-\epsilon^2)}{\epsilon} H^{(1)\prime}_{i\nu}(z) + \frac{(-2\epsilon^2+3)}{\epsilon^2}\frac{i}{\nu} H^{(1)}_{i\nu}(z)\right]
\end{aligned} \tag{C.27}$$

$$\begin{aligned}
\widehat{D_{33}} &= 4\epsilon\widehat{\cosh}(\xi) - \epsilon^2\widehat{\cosh}(2\xi) \\
&= -\frac{4\epsilon\pi}{2\omega}[H^{(1)}_{i\nu-1}(z) - H^{(1)}_{i\nu+1}(z)] + \frac{\epsilon^2\pi}{\omega}[H^{(1)}_{i\nu-2}(z) - H^{(1)}_{i\nu+2}(z)] \\
&= -\frac{4\epsilon\pi}{2\omega} 2H^{(1)\prime}_{i\nu}(z) + \frac{\epsilon^2\pi}{\omega}[\frac{4i\nu}{z} H^{(1)\prime}_{i\nu}(z) - \frac{4i\nu}{z^2} H^{(1)}_{i\nu}(z)] \\
&= \left(-\frac{4\epsilon\pi\eta}{\nu} + \frac{4\epsilon^2 i\pi\nu\eta}{i\nu^2\epsilon}\right) H^{(1)\prime}_{i\nu}(z) - \frac{4\epsilon^2 i\pi\nu\eta}{-\nu^3\epsilon^2} H^{(1)}_{i\nu}(z) \\
&= 4\pi\frac{\eta}{\nu}\frac{i}{\nu} H^{(1)}_{i\nu}(z)
\end{aligned} \tag{C.28}$$

$$
\begin{aligned}
\widehat{D_{12}} &= 6\epsilon\widehat{\sinh}(\xi) - 3\widehat{\sin}(2\xi) \\
&= -\frac{6\pi\epsilon}{2\omega}[H^{(1)}_{i\nu-1}(z) + H^{(1)}_{i\nu+1}(z)] + \frac{3\pi}{\omega}[H^{(1)}_{i\nu-2}(z) + H^{(1)}_{i\nu+2}(z)] \\
&= -\frac{6\pi\epsilon}{2\omega}\frac{2i\nu}{z}H^{(1)}_{i\nu}(z) + \frac{3\pi}{\omega}\left[\left(\frac{4(i\nu)^2}{z^2} - 2\right)H^{(1)}_{i\nu}(z) - \frac{4}{z}H^{(1)\prime}_{i\nu}(z)\right] \\
&= \left(\frac{3\pi}{\omega}\left(\frac{-4\nu^2}{-\nu^2\epsilon^2} - 2\right) - \frac{6\pi\epsilon i\nu\eta\epsilon}{i\nu^2\epsilon}\right)H^{(1)}_{i\nu}(z) - \frac{12\pi\eta}{i\nu^2\epsilon}H^{(1)\prime}_{i\nu}(z) \\
&= 12\pi\frac{\eta}{\nu}\frac{(1-\epsilon^2)}{\epsilon^2}H^{(1)}_{i\nu}(z) + 12\pi\frac{1}{\epsilon}\frac{i}{\nu}\frac{\eta}{\nu}H^{(1)\prime}_{i\nu}(z) \\
&= 12\pi\frac{1}{\epsilon}\frac{\eta}{\nu}i\left[\frac{(\epsilon^2-1)}{\epsilon}iH^{(1)}_{i\nu}(z) + \frac{1}{\nu}H^{(1)\prime}_{i\nu}(z)\right]
\end{aligned}
\tag{C.29}
$$

Appendix D

Source codes

D.1 Pyhton codes

```
import scipy as sc
from mpmath import *
mp.dps = 25; mp.pretty = True
import numpy as np
import matplotlib.pyplot as plt
from numpy import arange as xrange
from numpy import sin,cos,sinh,cosh,tan,tanh,arctan,arctanh,arccos

def dhank1(n,x):
        return (hankel1(n-1,x)-hankel1(n+1,x))/2


def PowerSpec(e,v):
    z = 1j*v*e
    S1 = v**4* np.absolute(3*(e**2-1)/e * dhank1(1j*v,z) \\
        +(e**2-3)/(e**2) *1j/v* hankel1(1j*v,z))**2
    S2 = v**4* np.absolute(3*(e**2-1)/e * dhank1(1j*v,z) \\
        + (2*e**2-3)/(e**2) *1j/v* hankel1(1j*v,z)) **2
    S3 = v**4* np.absolute(1j/v * hankel1(1j*v,z))**2
    S4 = v**4* 18*(e**2 -1)/(e**2) * np.absolute((e**2-1)/e \\
        * 1j*hankel1(1j*v,z)+ 1/v * dhank1(1j*v,z))**2
    return (S1+S2+S3+S4)


#Astro units
#-----------------------------------------------------
AU = 1.496*1e11 #m
MS = 1.988*1e30 #kg
# gravitational constant m^3/(kg s^2)
G = 6.674e-11
 #velocity of light
c = 299792458

#parameters for Hyperbolic trajactory
#-----------------------------------------------------
# velocity of m1 m/s
v0 = 0.1*c #7000
# impact parameter m
b = 5*1e-5 *AU #5e13
# masses kg
m1 = 30*MS #6e30
m2 =  m1      #1e28
m = m1 + m2 #total mass
```

```
ym = m1*m2/(m) #reduced mass
#angular momentum
L = b* v0 *ym
# eccentricity
e = np.sqrt(1+ (v0**4 * b**2)/(G**2 * m**2))
#a
a = (G*m)/v0**2
#alpha
alpha = G*m*ym
#n
n = np.sqrt((ym*a**3)/alpha)
#phi0
phi0 = np.arccos(-1/e)

print ('System parameters example')
print ('-------------------------------------------------------')
print ("Total mass:",m,"kg")
print ("Reduced mass:",ym,"kg")
print ("Eccentricity:",e )
print ("Impact b:",b,"m")
print ("a:",a)
print ("n:",n)
print ("phi0:",phi0)
print ()
print ('Numerical integration of the powerspectrum ')

Intnum =  sc.integrate.quad(lambda x:PowerSpec(e,x),0,70)
E_totnum = (G**(7/2) * m**(5/2) * ym**2 * 16 * np.pi**2)/(a**(7/2)\\
            * c**5 *180 * np.pi)*Intnum[0]
print ("Total emitted energy in GW of the hyperbolic encounter with e=",e)
print()
print ("Numerical Integration:",Intnum)
print ("E_tot:",E_totnum,'J')

print()
print ('Analytical calculation of the total energy for e:',e)
print()

def E_totana(G,L,b,c,ym,x0):
    return (G* L**5)/(90 * b**6 * c**5 * ym**3 *tan(x0)**2 * sin(x0)**4)\
             *(2628*x0 + 2328*x0*cos(2*x0)\
            +144*x0*cos(4*x0) -1948*sin(2*x0) -301*sin(4*x0))

E_totana = E_totana(G,L,b,c,ym,phi0)
print ('E_tot: ',E_totana,'J')
print ()

print ("Difference:",abs(E_totnum-E_totana),"J")
```

D.2 Mathematica codes

```
r1 := a * (ϵ^2 - 1) / (1 + ϵ * Cos[v - v0])
r2 := b * Sin[v0] / (Cos[v - v0] - Cos[v0])
r := a * (ϵ * Cosh[u] - 1)
x := a * (ϵ - Cosh[u])
y := a * Sqrt[ϵ^2 - 1] * Sinh[u]
t := n * (ϵ * Sinh[u] - u)
dudt := 1 / D[t, u]
dudt
M11 := μ * x^2
M22 := μ * y^2
M12 := μ * x * y
M11ttt := D[D[D[M11, u] * dudt, u] * dudt, u] * dudt
M22ttt := D[D[D[M22, u] * dudt, u] * dudt, u] * dudt
M12ttt := D[D[D[M12, u] * dudt, u] * dudt, u] * dudt
Simplify[M11ttt]
Simplify[M22ttt]
Simplify[M12ttt]
PD := M11ttt^2 + M22ttt^2 + 3 * M12ttt^2 - M11ttt * M22ttt
Simplify[PD, ϵ > 1]
```

$$\frac{1}{n\,(-1+\epsilon\,\text{Cosh}[u])}$$

$$-\frac{a^2\,\mu\,\left(4\,\left(-2+\epsilon^2\right)\,\text{Cosh}[u]+\epsilon\,\left(9-6\,\epsilon^2+\text{Cosh}[2\,u]\right)\right)\,\text{Sinh}[u]}{n^3\,(-1+\epsilon\,\text{Cosh}[u])^5}$$

$$-\frac{a^2\,\left(-1+\epsilon^2\right)\,\mu\,(-8\,\text{Cosh}[u]+\epsilon\,(7+\text{Cosh}[2\,u]))\,\text{Sinh}[u]}{n^3\,(-1+\epsilon\,\text{Cosh}[u])^5}$$

$$\frac{a^2\,\sqrt{-1+\epsilon^2}\,\mu\,\left(15\,\epsilon\,\text{Cosh}[u]+2\,\left(-4+\epsilon^2\right)\,\text{Cosh}[2\,u]+\epsilon\,(-10\,\epsilon+\text{Cosh}[3\,u])\right)}{2\,n^3\,(-1+\epsilon\,\text{Cosh}[u])^5}$$

$$\frac{2\,a^4\,\mu^2\,\left(-24+23\,\epsilon^2+\epsilon^2\,\text{Cosh}[2\,u]\right)}{n^6\,(-1+\epsilon\,\text{Cosh}[u])^6}$$

```
M11phi := μ * r2^2 * Cos[v]^2
M22phi := μ * r2^2 * Sin[v]^2
M12phi := μ * r2^2 * Sin[v] * Cos[v]
dphidt := L / (r2^2 * μ)
M11phittt := D[D[D[M11phi, v] * dphidt, v] * dphidt, v] * dphidt
M22phittt := D[D[D[M22phi, v] * dphidt, v] * dphidt, v] * dphidt
M12phittt := D[D[D[M12phi, v] * dphidt, v] * dphidt, v] * dphidt
Simplify[M11phittt]
Simplify[M22phittt]
Simplify[M12phittt]
PD := M11phittt^2 + M22phittt^2 + 3 * M12phittt^2 - M11phittt * M22phittt
Simplify[PD]
P := G / (45 c^5) * 6 * PD
Simplify[P]
```

$$\frac{1}{b^4 \mu^2} 2 L^3 \cos[v] (\cos[v - v0] - \cos[v0])^2 \cot[v0] \csc[v0]^3 (-4 \cos[v - v0] \sin[v] + 4 \cos[v0] \sin[v] + \cos[v] \sin[v - v0])$$

$$\frac{1}{b^4 \mu^2} 2 L^3 (\cos[v - v0] - \cos[v0])^2 \cot[v0] \csc[v0]^3 \sin[v] (4 \cos[v] (\cos[v - v0] - \cos[v0]) + \sin[v] \sin[v - v0])$$

$$\frac{1}{b^4 \mu^2} 2 L^3 \cot[v0] ((-1 + \cos[v]) \cot[v0] + \sin[v])^2 \left(2 \cos[v]^3 \cot[v0] - \cos[v] \cot[v0] \sin[v]^2 + 2 (\cot[v0] - \sin[v]) \sin[v]^2 + \cos[v]^2 (-2 \cot[v0] + \sin[v])\right)$$

$$\frac{1}{b^8 \mu^4} 32 L^6 (25 - 24 \cos[v] - 24 \cos[v - 2 v0] + 11 \cos[2 (v - v0)] + 12 \cos[2 v0]) \cot[v0]^2 \csc[v0]^6 \sin\left[\frac{v}{2}\right]^4 \sin\left[\frac{1}{2} (v - 2 v0)\right]^4$$

$$\frac{1}{15 b^8 c^5 \mu^4} 64 G L^6 (25 - 24 \cos[v] - 24 \cos[v - 2 v0] + 11 \cos[2 (v - v0)] + 12 \cos[2 v0]) \cot[v0]^2 \csc[v0]^6 \sin\left[\frac{v}{2}\right]^4 \sin\left[\frac{1}{2} (v - 2 v0)\right]^4$$

```
Integrate[(μ / L) P * r2^2, {v, 0, 2 * v0}]
```

$$\frac{1}{90 b^6 c^5 \mu^3} G L^5 \cot[v0]^2 \csc[v0]^4 (2628 v0 + 2328 v0 \cos[2 v0] + 144 v0 \cos[4 v0] - 1948 \sin[2 v0] - 301 \sin[4 v0])$$